

Table 1
Outcomes from non-animal photosafety testing.

No.	Chemical name	CAS number	Maximal MEC (M ⁻¹ cm ⁻¹) ^{a)}	ROS/mROS ^{b)}		3T3 NRU PT (PIF)	Photosafety information	
				Singlet oxygen (ΔA _{440 nm} · 10 ³)	Superoxide (ΔA _{560 nm} · 10 ³)		Phototoxic	Photoallergic
Phototoxins								
<i>Cosmetic ingredients</i>								
1	3,4',5-Tribromosalicylanilide	87-10-5	21,061 [325 nm]	81±2	<1	49.0	+	+
2	4-Methyl-7-ethoxycoumarin	87-05-8	15,509 [322 nm]	112±7	98±12	27.2		+
3	5-Methoxypsoralen	484-20-8	15,495 [311 nm]	65±18	424±3	229.9	+	–
4	6-Methylcoumarin	92-48-8	7,502 [290 nm]	196±11	112±8	21.3	+	+
5	7-Methoxycoumarin	531-59-9	15,255 [322 nm]	197±8	3±3	70.7		+
6	8-Methoxypsoralen	298-81-7	12,564 [299 nm]	143±13	8±8	120.5	+	+
7	Benzophenone	119-61-9	1,305 [290 nm]	227±21	<1	10.0		+
8	Bithionol	97-18-7	13,253 [307 nm]	273±22	<1	3.6	+	+
9	Dichlorophene	97-23-4	5,373 [290 nm]	213±4	<1	2.0		+
10	Fenticlor	97-24-5	10,002 [303 nm]	193±3	<1	1.4		+
11	Hexachlorophene	70-30-4	8,381 [298 nm]	437±5	<1	1.0	–	+
12	Methyl β-naphthylketone	93-08-3	7,691 [290 nm]	185±11	332±17	34.7	+	+
13	Methyl-N-methylanthranilate	85-91-6	6,248 [353 nm]	89±5	<1	168.2	+	
14	Musk ambrette	83-66-9	2,755 [290 nm]	224±2	<1	104.2	–	+
15	Musk ketone	81-14-1	350 [290 nm]	78±69	26±4	3.3	+	–
16	Musk xylene	81-15-2	448 [290 nm]	104±3	38±7	29.1	–	+
17	Octyl dimethyl PABA	21245-02-3	28,879 [310 nm]	76±3	158±9	2.7		+
18	p-Phenylenediamine	106-50-3	2,292 [310 nm]	153±14	<1	177.3		+
19	Tetrachlorosalicylanilide	1154-59-2	21,061 [325 nm]	74±1	<1	17.8	+	+
20	Triclocarban	101-20-2	3,342 [290 nm]	63±2	<1	1.0		+
<i>Non-cosmetics</i>								
21	Acridine	260-94-6	10,869 [355 nm]	274±26	229±18	1,782	+	–
22	Amiodarone HCl	19774-82-4	4,940 [290 nm]	301±5	209±4	2.7	+	
23	Anthracene	120-12-7	6,274 [357 nm]	99±6	403±10	6,666	+	–
24	Chlorpromazine HCl	69-09-0	6,222 [307 nm]	231±9	<1	9.2	+	+
25	Diclofenac Na	15307-79-6	8,747 [290 nm]	473±21	343±15	1.3	+	+
26	Enoxacin	74011-58-8	12,063 [345 nm]	516±30	271±24	119.0		+
27	Fenofibrate	49562-28-9	13,045 [290 nm]	477±12	188±11	363.6	+	
28	Indomethacin	53-86-1	8,738 [290 nm]	29±13	168±18	1.5	+	
29	Ketoprofen	22071-15-4	2,780 [290 nm]	316±8	106±5	75.4	–	+
30	Piroxicam	36322-90-4	22,389 [327 nm]	181±29	204±17	1.0		+
31	Promethazine HCl	58-33-3	4,400 [298 nm]	245±12	<1	8.3	+	+
32	Quinine HCl (2 H ₂ O)	6119-47-7	4,451 [331 nm]	510±9	381±5	15.7	+	+
33	Sulfanilamide	63-74-1	3,677 [290 nm]	265±19	41±4	1.0		+
34	Tetracycline HCl	64-75-5	12,163 [355 nm]	399±16	150±11	28.8	+	
Non-phototoxic chemicals								
<i>Cosmetic ingredients</i>								
35	1,3-Butylene glycol	107-88-0	<10	<1	<1	1.0	–	–
36	2-Propanol	67-63-0	<10	6±4	<1	1.0	–	–
37	4'-Methylbenzylidene camphor	36861-47-9	11,876 [299 nm]	<1	<1	1.0	–	–
38	Ascorbic acid	50-81-7	773 [290 nm]	237±4	71±6	1.0	–	–
39	Cetyl alcohol	36653-82-4	<10	5±7	<1	1.0	–	–
40	Ethanol	64-17-5	<10	<1	<1	1.0	–	–
41	Glycerine	56-81-5	<10	<1	<1	1.0	–	–
42	Isopropyl myristate	110-27-0	<10	5±9	<1	1.0	–	–
43	Lauric acid	143-07-7	<10	3±4	13±2	1.7	–	–
44	Propylene glycol	57-55-6	<10	<1	<1	1.0	–	–
45	Sodium laurate	629-25-4	<10	1±6	7±6	1.3	–	–
46	Sodium lauryl sulfate	151-21-3	<10	<1	<1	1.0	–	–
47	Sulisobenzone	4065-45-6	15,790 [290 nm]	<1	<1	1.0	–	–
<i>Non-cosmetics</i>								
48	DMSO	67-68-5	<10	12±25	11±23	1.0	–	–
49	Lactic acid	50-21-5	<10	10±20	<1	1.0	–	–
50	Methyl salicylate	119-36-8	4,722 [308 nm]	25±12	<1	1.0	–	–
51	Penicillin G	113-98-4	31 [318 nm]	20±24	9±21	1.0	–	–

a) Plain letters: MEC values at λ_{max} observed between 290–700 nm; and italic letters: MEC values at 290 nm (shoulders). b) Plain letters: ROS data at 200 μM; italic letters in open box: mROS assay at 200 μM; in gray box: 100 μM; and in black box: 50 μM.

subjected to the mROS assay (Seto et al., 2013). Briefly, singlet oxygen was measured in an aqueous solution by spectrophotometrically monitoring the bleaching of *p*-nitrosodimethylaniline at 440 nm using imidazole as a selective acceptor of singlet oxygen. Samples, containing the tested chemical (200 μM), *p*-nitrosodimethylaniline (50 μM) and imidazole (50 μM) in 20 mM sodium phosphate buffer (NaPB, pH 7.4), were mixed in a tube. Two hundred microliters of the sample was transferred into a well of a plastic 96-well plate (Asahi Glass Co., Ltd., Tokyo, Japan; code number: 3881-096; clear, untreated, flat-bottomed) and checked for precipitation before light exposure. The plate was subjected to the measurement of absorbance at 440 nm using a SAFIRE microplate spectrophotometer (TECAN, Mannedorf, Switzerland).

The plate was fixed in a quartz reaction container with a quartz cover, and then irradiated with simulated sunlight for 1 h. After agitation on a plate shaker, the UV absorbance at 440 nm was measured. For the determination of superoxide, samples containing the tested chemical (200 μM) and NBT (50 μM) in 20 mM NaPB were irradiated with simulated sunlight for 1 h, and the reduction in NBT was measured by the increase in absorbance at 560 nm in the same manner as the singlet oxygen determination.

2.3.3. mROS assay

Since some chemicals were non-testable in the ROS assay due to limited aqueous solubility, mROS assay was carried out using a micellar solution of 0.5% (v/v) Tween 20 (Seto et al., 2013).

The critical micelle concentration (CMC) of Tween 20 was ca. 0.005% (v/v) in distilled water (Wan and Lee, 1974), and the applied concentration of Tween 20 for the mROS assay was almost identical to 100-fold of the CMC. Briefly, to monitor the generation of singlet oxygen, compounds (200 μM), *p*-nitrosodimethylaniline (50 μM) and imidazole (50 μM) were dissolved in 20 mM NaPB (pH 7.4) with 0.5% (v/v) Tween 20. For the determination of superoxide generation, compounds (200 μM) and NBT (50 μM) were dissolved in 20 mM NaPB (pH 7.4) with 0.5% (v/v) Tween 20. Then, these samples were irradiated with simulated sunlight and measured under the same conditions with the ROS assay protocol. All samples were checked for precipitation by visual observation before and after light exposure. According to the results of preliminary study, Tween 20 was found to be a weak ROS generator (data not shown), so the results were calculated by subtracting blank readings from sample readings.

2.4. 3T3 NRU PT

The *in vitro* 3T3 NRU PT was carried out as described in the Organisation for Economic Co-operation and Development (OECD) 432 guidelines and the European Community Official Journal (L 136/9, 08.06.2000, annexe II) with minor modification. Briefly, Balb/c 3T3 cells were maintained in culture for 24 h for formation of monolayers. Two 96-well plates per test chemical were then pre-incubated with six different concentrations of the chemical in duplicates for 1 h. One plate was then exposed to a dose of 5 J/cm² UVA (+Irr experiment), whereas the other plate was kept in the dark (–Irr experiment). UVA irradiation was performed using a SOL 500 Sun Simulator (Dr. Hönle AG UV Technology) equipped with a 500 W metal halide lamp and an H1 filter to attenuate UVB. The treatment medium was then replaced with culture medium and, after 24 h, cell viability was determined by neutral red uptake for 3 h. The neutral red uptake was measured at the absorbance of 540 nm using the Benchmark™ Plus microplate spectrophotometer (BioRad, Hercules, CA, USA). Cell viability obtained with each of the six concentrations of the test chemical was compared with that of untreated controls and the percent inhibition was calculated. For prediction of phototoxic potential, the concentration responses obtained in the presence and in the absence of UV irradiation were compared, usually at the IC₅₀ level, that is, the concentration inhibiting cell viability by 50% of that of the untreated controls. The photoirritation factor (PIF) was determined as follows:

$$\text{PIF} = \frac{\text{IC}_{50}(-\text{Irr})}{\text{IC}_{50}(+\text{Irr})}$$

2.5. Statistical analysis

For statistical comparisons, one-way analysis of variance (ANOVA) with pairwise comparison by Fisher's least significant difference procedure was used. A *P* value of less than 0.05 was considered significant for all analyses.

3. Results and discussion

3.1. UV/VIS spectral analysis

In general, the absorption of sunlight by the chromophore moiety of a phototoxin is responsible for its excitation, so UV/VIS absorption has been believed to be a key indicator of photosafety (Henry et al., 2009). As the Grotthus–Draper law of photobiology states, only light that is absorbed can be active in photochemical and photobiological processes (Onoue et al., 2009). To clarify the photoreactivity of tested chemicals, UV/VIS spectral analysis was carried out for all the tested chemicals (Fig. 1 and Table 1). For

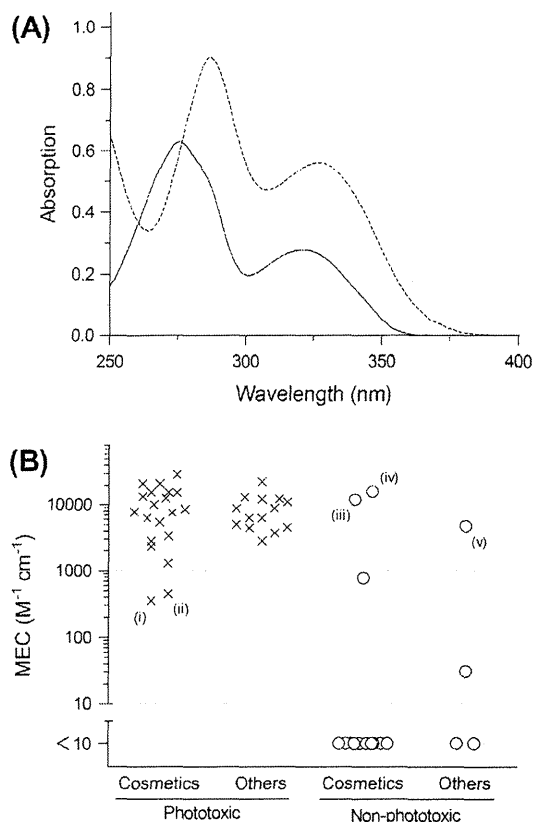


Fig. 1. UV/VIS absorption of tested chemicals. (A) Spectral patterns of 6-methylcoumarin (**4**: 50 μM , solid line) and sulisobenzene (**47**: 50 μM , dashed line) in ethanol. (B) MEC values of tested chemicals. x, phototoxins; and o, non-phototoxic chemicals. (i) Musk ketone (**15**), (ii) musk xylene (**16**), (iii) 4'-methylbenzylidene camphor (**37**), (iv) sulisobenzene (**47**) and (v) methyl salicylate (**50**).

instance, 6-methylcoumarin (**4**), a synthetic fragrance with high phototoxic potential, and sulisobenzene (**47**), a non-phototoxic sunscreen, exhibited intense absorption in UVA and B regions (Fig. 1A), and no absorption was seen in the VIS region (data not shown). Maximal MEC values of 6-methylcoumarin (**4**) and sulisobenzene (**47**) within the UV/VIS region were calculated to be 7502 M⁻¹ cm⁻¹ (290 nm) and 15790 M⁻¹ cm⁻¹ (290 nm), respectively. Henry and co-workers previously demonstrated that chemicals with a MEC of less than 1000 M⁻¹ cm⁻¹ were less of a phototoxic risk (Henry et al., 2009). According to this tentative threshold of MEC value, it cannot be denied that both cosmetic ingredients have low phototoxic risk, whereas sulisobenzene (**47**) was identified to be non-phototoxic in humans. In addition to these two model cosmetics, phototoxic risks of other cosmetics, drugs and food additives were assessed on the basis of UV/VIS-absorbing properties (Fig. 1B). In the 18 non-cosmetic chemicals, there were no false-negative predictions, and only methyl salicylate (**50**) within non-phototoxic group exhibited intense UV absorption with an MEC value of 4722 M⁻¹ cm⁻¹ (308 nm). Thus, the classification threshold (1000 M⁻¹ cm⁻¹) using MEC seemed to be efficacious for photosafety assessment of non-cosmetic chemicals. However, MEC data on cosmetics were partly misleading, providing false-negative predictions on musk ketone (**15**) and musk xylene (**16**) and false-positive predictions on 4'-methylbenzylidene camphor (**37**) and sulisobenzene (**47**). It was not surprising that false-positive predictions occurred since some non-phototoxic chemicals have intense UV/VIS absorption (Onoue and Tsuda, 2006); however, musk ketone (**15**) and musk xylene (**16**) were expected to be potent UV/VIS absorbers since they have

been recognized as a phototoxin and a photoallergen, respectively (SCCNFP, 2004). The MEC values of these two phototoxins were found to be less than $500 \text{ M}^{-1} \text{ cm}^{-1}$; therefore, the defined threshold ($1000 \text{ M}^{-1} \text{ cm}^{-1}$) might not always be reliable for photosafety testing of cosmetics. The positive/negative predictivities of an MEC-based approach were calculated to be 85.7%/83.3% for cosmetics and 93.3%/100% for non-cosmetic chemicals. In addition, the sensitivity and specificity were found to be 90% and 76.9% for cosmetics and 100% and 75% for non-cosmetic chemicals.

3.2. ROS assay

3.2.1. Assay applicability to cosmetics

Because of the few false-negative predictions in the MEC-based approach, combination use of other photosafety testing might be needed to ensure the photosafety of cosmetics. Previously, ROS assay was developed for photosafety assessment of pharmaceutical substances (Onoue et al., 2008b; Onoue and Tsuda, 2006), in which the generation of ROS such as singlet oxygen and superoxide from photoirradiated chemicals was monitored. Then, for further photochemical characterization, the ROS assay was applied to the chemicals. Validation study on the ROS assay has been carried out by the Japan Pharmaceutical Manufacturers Association (JPMA), supervised by the Japanese Center for the Validation of Alternative Methods (JaCVAM), to verify relevance and reliability (Onoue et al., 2013). In accordance with the validated protocol, most non-cosmetic chemicals seemed to be evaluable in the ROS assay, whereas assays on some cosmetics were unscreenable for two major reasons: (i) apparent color change of the assay solution during exposure to simulated sunlight, and (ii) limited solubility in aqueous media.

3.2.2. Spectral interference of discoloring cosmetics in ROS determination

Assay solution of *p*-phenylenediamine (**18**), a hair dye, exhibited intense coloring during light exposure, and the color transition might lead to severe spectral interference at defined wavelength numbers for determination of singlet oxygen (440 nm) and superoxide (560 nm). To clarify possible interference in ROS determination, *p*-phenylenediamine (**18**), dissolved in 20 mM NaPB (pH 7.4), was exposed to simulated sunlight (ca. 2.0 mW/cm^2) for up to 60 min, and the UV/VIS spectral patterns of irradiated *p*-phenylenediamine (**18**) solution were measured (Fig. 2A). In its intact form, no significant absorption was seen in the VIS region; however, exposure of *p*-phenylenediamine (**18**) to the simulated sunlight resulted in gradual coloring in the VIS region. Although

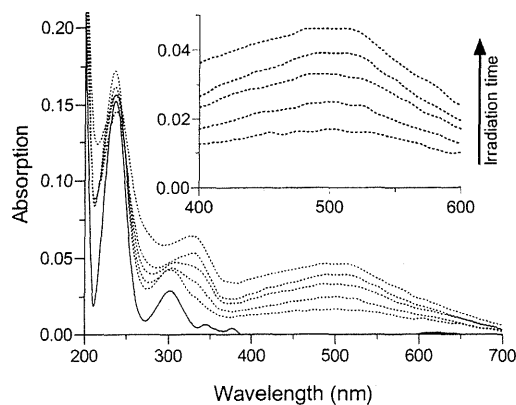


Fig. 2. UV-transition of *p*-phenylenediamine (**18**) during light exposure. Solid line, intact *p*-phenylenediamine (**18**, 20 μM) dissolved in 20 mM NaPB; and dotted line, after exposure to simulated sunlight (ca. 2.0 mW/cm^2) for 5, 10, 15, 30 and 60 min.

detailed photoproducts of *p*-phenylenediamine (**18**) in the current study are still unclear, in the previous photostability testing, the main photochemical product was deduced to be dimer [2-(4'-aminoanilino)-5-hydroxy-1,4-quinonediimine] or trimer Bandrowski's base [4-diamine,3,6-bis((*p*-aminophenyl)imino)-4-cyclohexadiene-1] with potent UV/VIS absorption (Nishi and Nishioka, 1982). From these observations, photochemical degradation of *p*-phenylenediamine (**18**) and other discoloring cosmetics during ROS assay might have had a major impact on the reliability of assay outcomes because of spectral interference. Therefore, as well as ROS assay solution, each tested chemical dissolved in assay buffer without ROS-measuring reagents was also exposed to the simulated sunlight as an experimental control, and results were calculated by subtracting control readings from sample readings with the aim of minimizing spectral interference. In the validated ROS assay protocol, ROS data on *p*-phenylenediamine (**18**) were calculated to be <1 for singlet oxygen ($\Delta A_{440 \text{ nm}} \times 10^3$) and 81 ± 19 for superoxide ($\Delta A_{560 \text{ nm}} \times 10^3$), and the assay outcomes were quite different in accordance with the modified assay protocol {singlet oxygen ($\Delta A_{440 \text{ nm}} \times 10^3$), 153 ± 14 ; and superoxide ($\Delta A_{560 \text{ nm}} \times 10^3$), <1 }. Since some cosmetic chemicals, especially dyes and sunscreens, have intense VIS absorption even before UV exposure, the newly proposed assay protocol employing an experimental control might be suitable for the reliable photosafety assessment of cosmetics.

3.2.3. Solubility issue

The modified assay protocol was applied to all the tested chemicals (**1–51**) (Table 1), and 14 cosmetic ingredients (ca. 42% of total cosmetic chemicals) and 3 non-cosmetic chemicals (ca. 17% of total non-cosmetics) were found to be still non-testable because of limited solubility. To overcome this problem, our group previously proposed the optional use of albuminous and micellar solution for ROS assay on poorly water-soluble chemicals (Onoue et al., in press-b; 2008c; Seto et al., 2013). Although previous study demonstrated a very few false-negatives predictions in the mROS assay (Seto et al., 2013), complementary use of mROS assay could strengthen the assay performance of the ROS assay for a wide range of new drug candidates for exploratory and regulatory purposes. The assay buffer for mROS assay could dissolve 14 non-testable chemicals at a final concentration of 200 μM . In contrast, 3,4,5-tribromosalicylanilide (**1**), tetrachlorosalicylanilide (**19**) and anthracene (**23**) were still poorly soluble even in the micellar solutions, and thus they were assessed at diluted concentrations (50 μM or 100 μM). From these findings, the optional use of mROS assay achieved a marked increase in the number of evaluable compounds compared with the ROS assay alone.

3.2.4. Prediction capacity

In theory, excitation of the drug by UV/VIS light may give rise to ROS, which may be one of causative agents for the drug-induced phototoxicity through oxidative damage of cellular membrane, DNA and other biomolecules (Brendler-Schwaab et al., 2004; Epstein and Wintroub, 1985). In addition to these phototoxic responses, there is also the probability that the photochemical reaction of compounds with ROS resulted in the yield of some toxic degradants. For some drugs, such as amiodarone and chlorpromazine, metabolites may play a significant role in phototoxic responses (Ferguson et al., 1985; Ljunggren and Moller, 1977). These photochemical events in the early stage of phototoxicity would provide a rationale for determination of ROS generated from the photoirradiated chemicals for photosafety assessment. In the ROS/mROS assays (Table 1), there appeared to be significant ROS generation from both cosmetic and non-cosmetic phototoxins (200 μM) under exposure to simulated sunlight (Table 1), and anthracene (**23**) was found to be a potent ROS generator even at 50 μM in the mROS as-

↑ Photoreactivity (+) ↓ Phototoxicity (-)	[ROS] 20	[ROS] 2
	with [mROS] 34	with [mROS] 2
	[ROS] 0	[ROS] 12
	with [mROS] 0	with [mROS] 15

Fig. 3. Prediction capacity of ROS assay with or without follow-up mROS assay for the *in vitro/in vivo* photosafety of tested chemicals.

say. Interestingly, both musk ketone (**15**) and musk xylene (**16**) exhibited potent ROS generation, whereas they were weak UV/VIS absorbers with MEC values below $500 \text{ M}^{-1} \text{ cm}^{-1}$. In contrast, non-phototoxic chemicals tended to show weak ROS generation. Previous investigation demonstrated that the photoreactivity of compounds tested at $200 \mu\text{M}$ could be predicted according to the discrimination criteria of ROS data ($25 (\Delta A_{440 \text{ nm}} \times 10^3)$ for singlet oxygen and $20 (\Delta A_{560 \text{ nm}} \times 10^3)$ for superoxide) (Onoue et al., 2008a). In addition, these criteria would still be available for positive prediction of the diluted samples in the mROS assay; however, negative predictions would be challenging under dilution since some diluted phototoxins might exhibit weak ROS generation. Herein, careful consideration should be made on negative predictivity for the diluted samples, and the diluted samples with a subthreshold level should be identified to be non-testable in the mROS assay. According to these criteria, only 20 out of 34 phototoxins (ca. 59%) can be identified to be phototoxic in the ROS assay, and optional application of the mROS assay to those non-testable chemicals (**1**, **3**, **9**, **10**, **14–20**, **22**, **23** and **27**) could achieve positive prediction on all tested phototoxins (Fig. 3). In 13 non-phototoxic cosmetics, 3 chemicals (ca. 23%; **37**, **42** and **46**) were non-testable in the ROS assay on the basis of visual inspection of precipitation. They could be assessed in the mROS assay at $200 \mu\text{M}$, and most of them exhibited weak ROS generation below the criteria. On the basis of combined use of the ROS and mROS assays, photosafety prediction on all tested chemicals could be achieved with individual specificity, positive and negative predictivities of 88.2%, 94.4% and 100%, respectively. The ROS and optional mROS assays did not provide any false-negative predictions for both cosmetics and non-cosmetics, whereas unexpectedly ascorbic acid (**38**) was falsely predicted to be photoreactive/phototoxic according to significant ROS generation (singlet oxygen ($\Delta A_{440 \text{ nm}} \times 10^3$), 237 ± 4 ; and superoxide ($\Delta A_{560 \text{ nm}} \times 10^3$), 71 ± 6). In the ROS assay, superoxide can be measured upon the reduction of nitroblue tetrazolium, and determination of singlet oxygen can be made on the basis of bleaching of *p*-nitrosodimethylaniline by oxidized imidazole (Onoue and Tsuda, 2006). Ascorbic acid (**38**) and other reducing substances reduced the tetrazolium salt to a formazan directly (Bruggisser et al., 2002), and ascorbic acid (**38**) also accelerated the oxidation of imidazole derivatives (Imanaga, 1955). The data discrepancy on ascorbic acid (**38**) might be partly explained by the interference in the ROS assay through these chemical reactions. Some skin-lightening cosmetics may have potent reducing properties, so the chemical interference with ROS determination could be an assay limitation in the ROS assay for cosmetic ingredients.

Currently, in the International Conference on Harmonization of Technical Requirements for Registration of Pharmaceuticals for Human Use (ICH), introduction of the validated ROS assay in the photosafety guidelines is under consideration (ICH S10 Guideline: "Photosafety Evaluation of Pharmaceuticals"). From the present

findings, in spite of some assay limitations, the ROS assay might also be applicable to the photosafety assessment of cosmetics in combination with the mROS assay for non-testable chemicals with low solubility.

3.3. 3T3 NRU PT

The 3T3 NRU PT was developed and validated under the auspices of European Centre for the Validation of Alternative Methods (ECVAM) to establish a valid *in vitro* alternative to the various *in vivo* phototoxicity tests (Liesch and Spielmann, 2002). The test is now accepted by the European Union commission and member states as being necessary for all compounds showing absorbance of UVA and visible light (Onoue et al., 2009). Herein, all chemicals were assessed in the 3T3 NRU PT for further clarification of the photosafety of cosmetics using the Balb/c 3T3 mouse fibroblast cell line (Table 1). The 3T3 NRU PT assesses the cytotoxic effect of a test substance after exposure to a non-cytotoxic dose of UVA light compared with that in the absence of exposure, and the cytotoxicity is expressed as a concentration-dependent reduction of the uptake of the vital dye – Neutral Red (Fig. 4A). Under UVA exposure to 6-methylcoumarin (**4**), the cell viability was shifted to lower

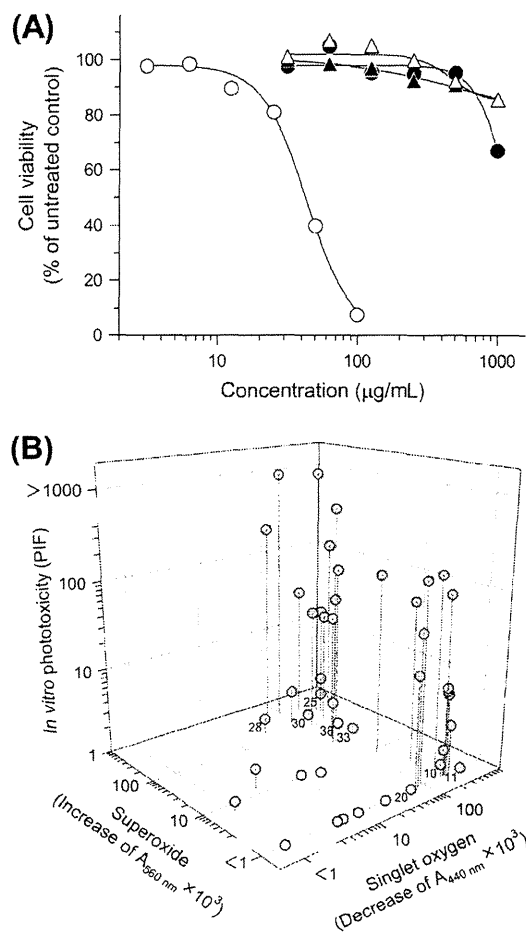


Fig. 4. 3T3 NRU phototoxicity testing and its relevance to ROS assay. (A) Photosafety of 6-methylcoumarin (**4**) and sulisobenzone (**47**) in the 3T3 NRU PT. Data represent mean for 3–4 experiments. ●, 6-methylcoumarin (**4**) without UVA; ○, with UVA; ▲, sulisobenzone (**47**) without UVA; and △, with UVA. (B) A 3D-plot of ROS data versus 3T3 NRU PT data for 51 compounds. ○, non-phototoxic chemicals; and ●, phototoxins. Some data are highlighted with chemical identification numbers.

concentrations, in which the IC_{50} values with and without UV irradiation were 46.5 $\mu\text{g}/\text{mL}$ and 988.3 $\mu\text{g}/\text{mL}$, respectively. These values produced a PIF of 21.3 for 6-methylcoumarin (**4**). PIF values are effective to discriminate phototoxic molecules ($PIF \geq 5$) from non-phototoxic ones, but were actually unable to discriminate correctly between mildly or probably phototoxic molecules ($2 \leq PIF < 5$) and non-phototoxic ones ($PIF < 2$). According to the classification criteria of PIF values, 6-methylcoumarin (**4**) was deduced to be phototoxic. In contrast, sulisobenzone (**47**) could be identified as not phototoxic since no significant differences were seen in cell viability curves between UVA-irradiated and non-irradiated groups, providing a PIF value of ca. 1. Most cosmetic and non-cosmetic phototoxins, especially 5-methoxypsoralen (**3**), acridine (**21**), anthracene (**23**) and fenofibrate (**27**), exhibited high PIF values (>200), and these observations were in agreement with outcomes from the UV/VIS spectral analysis and ROS assay (Table 1). A 3D plot of ROS data versus PIF values for the 51 tested compounds is presented in Fig. 4B, in which red and blue circles indicate phototoxic and non-phototoxic chemicals, respectively. Although all phototoxins were potent ROS generators, low PIF values (<2) were seen for some chemicals, including fenticlor (**10**), hexachlorophene (**11**) and triclocarban (**20**) as cosmetics, and diclofenac Na (**25**), indomethacin (**28**), piroxicam (**30**) and sulfanilamide (**33**) as pharmaceutical substances. In the 3T3 NRU PT, a UVA light source is basically used since 3T3 cells cannot resist higher doses of UVB light, so the 3T3 NRU PT tends to provide false-negative prediction for chemicals predominantly or solely absorbing in the UVB range (Ceridono et al., 2012). Both diclofenac Na (**25**) and sulfanilamide (**33**) were UVB absorbers with MEC values (320 nm) of $327 \text{ M}^{-1} \text{ cm}^{-1}$ and $42 \text{ M}^{-1} \text{ cm}^{-1}$, respectively, which might explain in part the false prediction. Fenticlor (**10**), hexachlorophene (**11**), piroxicam (**30**) and sulfanilamide (**33**) have been recognized as potent photoallergens, so they would not be captured by the 3T3 NRU PT since this assay system was originally developed to detect the photoirritant potential of a drug and is not designed to predict other adverse effects that may arise from the combined action of a chemical and light, for example, photogenotoxicity, photoallergy and photocarcinogenicity (Onoue et al., 2009). The exact reasons for the data discrepancy are still uncertain, and further accumulation of data might provide further insight into assay limitations

and the applicability domain. Thus, the 3T3 NRU PT provided false-negative predictions in the present study, and sensitivity, individual specificity, positive and negative predictivities of the 3T3 NRU PT on the 51 tested chemical were calculated to be 79.4%, 100%, 100% and 70.8%, respectively.

3.4. Proposed testing approach for cosmetic chemicals

In the present study, the photosafety of 33 cosmetic and 18 non-cosmetic chemicals was assessed by *in vitro* photochemical and photobiochemical screenings, the strategic use of which was already proposed for photosafety testing on pharmaceutical substances in the ICH S10 draft guideline (ICH, 2013). All photosafety testing was partly applicable to photosafety assessment of the cosmetics, although some modifications of the test protocol and decision criteria were needed for reliable screening of cosmetics. On the basis of the outcomes from the present study, a tiered testing approach was proposed for non-animal photosafety assessment of cosmetic ingredients (Fig. 5).

Since absorption of UV/VIS light by a phototoxin would be a key trigger of phototoxic events, MEC-based photosafety testing might be available as first screening in the tiered photosafety testing. In the present study, the MEC values of some cosmetics were at a sub-threshold level ($<1000 \text{ M}^{-1} \text{ cm}^{-1}$), providing false-negative predictions in UV/VIS spectral analysis. A reduced threshold value would be preferable to allow reliable photosafety testing on cosmetics, and the MEC value of $100 \text{ M}^{-1} \text{ cm}^{-1}$ seemed to be effective with no false-negatives in the present study. Further accumulation of substantial MEC data of cosmetics should lead to the proposal of a new threshold with high predictivity. Next, as second screening, the ROS assay would be efficacious for monitoring actual photochemical responses for tested chemicals with an MEC value over $100 \text{ M}^{-1} \text{ cm}^{-1}$. In the ROS assay, there appeared to be severe spectral interference in the determination of ROS from some cosmetic phototoxins, and ca. 42% of cosmetics were non-testable because of limited solubility. To avoid spectral interference of discoloring cosmetics in ROS determination, an experimental control was employed upon exposure of tested chemical alone to simulated sunlight, to subtract control readings from sample readings. The mROS assay could be employed for follow-up screening on the

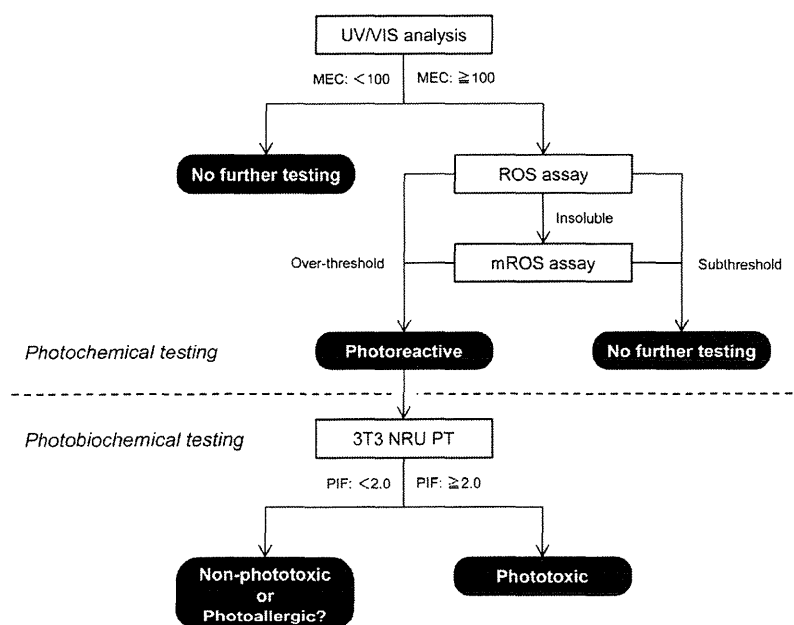


Fig. 5. Proposed non-animal photosafety assessment approaches for cosmetics.

non-testable samples with poor solubility, as evidenced by the fact that all the tested chemicals could be assessed by the combination use of ROS and mROS assays in the present study. If the tested chemicals were found to be less photoreactive in the ROS and mROS assays, no further testing would be needed. The potent ROS generators would be assessed by the 3T3 NRU PT in terms of *in vitro* phototoxicity basically in accordance with OECD test guideline 432, and the tested chemical could be defined as phototoxic, probably phototoxic, or not phototoxic using the validated criteria. The 3T3 NRU PT was originally designed for the identification of phototoxicity, not for photoallergy (Onoue et al., 2009), although some photoallergens might react positively in the 3T3 NRU PT. There is no denying that the tested chemicals might be photoallergic even though they were judged not to be phototoxic in the 3T3 NRU PT (Liebsch and Spielmann, 2002). In this study, the 3T3 NRU PT provided negative predictions on some photoallergens (**10**, **11**, **20**, **30** and **33**), although they were found to be positive in both UV/VIS analysis and ROS assay. Therefore, further appropriate assessments should be made to clarify the photoallergic potential of tested chemicals as long as they exhibit potent photoreactivity. Recent investigations demonstrated high screening performance of a photo human cell line activation test (photo-h-CLAT) and pig skin model for photoallergic prediction, although the assays have not been internationally accepted (Seto et al., 2012). In addition, careful interpretation of assay outcomes should be made on the UVB absorbers since they might not be captured in the 3T3 NRU PT. On the basis of the present outcomes, the complementary use of *in vitro* photochemical and photobiochemical testing would be effective in non-animal photosafety assessment of cosmetic chemicals, as well as drugs, food and other chemicals.

4. Conclusion

The present study demonstrated the limited predictivity and applicability of each non-animal photosafety testing, such as UV/VIS spectral analysis, ROS assay and 3T3 NRU PT, for cosmetic ingredients. Taking into account their assay principles and the applicability domain, a tiered testing approach for non-animal photosafety evaluation was proposed with combination use of *in vitro* photosafety testing methods. The proposed assay strategy would meet the 3R requirements in the sense of “reduction” and “replacement” of animal testing, and the assay outcomes would be available for the development of cosmetic products with a wide safety margin.

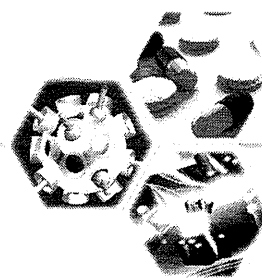
Conflict of Interest

None of the authors have any conflicts of interest associated with this study.

References

- Adler, S., Basketter, D., Creton, S., Peikonen, O., van Benthem, J., Zuang, V., Andersen, K.E., Angers-Loustau, A., Aptula, A., Bal-Price, A., Benfenati, E., Bernauer, U., Bessems, J., Bois, F.Y., Boobis, A., Brandon, E., Bremer, S., Broschard, T., Casati, S., Coecke, S., Corvi, R., Cronin, M., Daston, G., Dekant, W., Felton, S., Grignard, E., Gundert-Reyny, U., Heinonen, T., Kimber, I., Kleijnans, J., Komulainen, H., Kreiling, R., Kreysa, J., Leite, S.B., Loizou, G., Maxwell, G., Mazzatarra, P., Munn, S., Pihler, S., Phrakonkham, P., Piersma, A., Poth, A., Prieto, P., Repetto, G., Rogiers, V., Schoeters, G., Schwarz, M., Serafimova, R., Tahli, H., Testai, E., van Delft, J., van Loveren, H., Vinken, M., Worth, A., Zaldivar, J.M., 2011. Alternative (non-animal) methods for cosmetics testing: current status and future prospects-2010. *Arch. Toxicol.* **85**, 367–485.
- Allen, S.K., Todd, A., Allen, J.M., 1997. Photochemical formation of singlet molecular oxygen (1O_2) in illuminated 6-methylcoumarin solutions. *Biochem. Biophys. Res. Commun.* **235**, 615–618.
- Balls, M., Clotier, R., 2010. A FRAME response to the Draft Report on Alternative (Non-animal) methods for cosmetics testing: current status and future prospects-2010. *Altern. Lab. Anim.* **38**, 345–353.
- Brendler-Schwaab, S., Czich, A., Epe, B., Gocke, E., Kaina, B., Muller, L., Pollet, D., Utesch, D., 2004. Photochemical genotoxicity: principles and test methods. Report of a GUM task force. *Mutat. Res.* **566**, 65–91.
- Bruggisser, R., von Daeniken, K., Jundt, G., Schaffner, W., Tullberg-Reinert, H., 2002. Interference of plant extracts, phytoestrogens and antioxidants with the MTT tetrazolium assay. *Planta. Med.* **68**, 445–448.
- Ceridono, M., Tellner, P., Bauer, D., Barros, J., Alepee, N., Corvi, R., De Smedt, A., Fellows, M.D., Gibbs, N.K., Heisler, E., Jacobs, A., Jirova, D., Jones, D., Kandarova, H., Kasper, P., Akunda, J.K., Krul, C., Learn, D., Liebsch, M., Lynch, A.M., Muster, W., Nakamura, K., Nash, J.F., Pfannenbecker, U., Phillips, G., Robles, C., Rogiers, V., Van De Water, F., Liminga, U.W., Vohr, H.W., Watrelos, O., Woods, J., Zuang, V., Kreysa, J., Wilcox, P., 2012. The 3T3 neutral red uptake phototoxicity test: practical experience and implications for phototoxicity testing – the report of an ECVAM-EFPIA workshop. *Regul. Toxicol. Pharmacol.* **63**, 480–488.
- The European Agency for the Evaluation of Medicinal Products, Evaluation of Medicines for Human Use, Committee for Proprietary Medicinal Products (EMA/CPMP), 2002. Note for Guidance on Photosafety Testing, CPMP/SWP/398/01.
- Epstein, J.H., 1983. Phototoxicity and photoallergy in man. *J. Am. Acad. Dermatol.* **8**, 141–147.
- Epstein, J.H., Wintroub, B.J., 1985. Photosensitivity due to drugs. *Drugs* **30**, 42–57.
- The Food and Drug Administration, Center for Drug Evaluation and Research (FDA/CDER), 2002. Guidance for Industry, Photosafety Testing.
- Ferguson, J., Addo, H.A., Jones, S., Johnson, B.E., Frain-Bell, W., 1985. A study of cutaneous photosensitivity induced by amiodarone. *Br. J. Dermatol.* **113**, 537–549.
- Henry, B., Fori, C., Alsanje, K., 2009. Can light absorption and photostability data be used to assess the photosafety risks in patients for a new drug molecule? *J. Photochem. Photobiol. B* **96**, 57–62.
- Hoya, M., Hirota, M., Suzuki, M., Hagino, S., Itagaki, H., Aiba, S., 2009. Development of an *in vitro* photosensitization assay using human monocyte-derived cells. *Toxicol. In Vitro* **23**, 911–918.
- International Conference on Harmonization of Technical Requirements for Registration of Pharmaceuticals for Human Use (ICH), 2013. ICH Guideline S10 Guidance on Photosafety Evaluation of Pharmaceuticals (draft).
- Imanaga, Y., 1955. Autooxidation of L-ascorbic acid and imidazole nucleus. *J. Biochem.* **42**, 657–667.
- Liebsch, M., Spielmann, H., 2002. Currently available *in vitro* methods used in the regulatory toxicology. *Toxicol. Lett.* **127**, 127–134.
- Ujungren, B., Moller, H., 1977. Phenothiazine phototoxicity: an experimental study on chlorpromazine and its metabolites. *J. Invest. Dermatol.* **68**, 313–317.
- Lovell, W.W., Jones, P.A., 2000. Evaluation of mechanistic *in vitro* tests for the discrimination of photoallergic and photoirritant potential. *Altern. Lab. Anim.* **28**, 707–724.
- Maxwell, G., Aebly, P., Ashikaga, T., Bessou-Touya, S., Diembeck, W., Gerberick, F., Kern, P., Marrec-Fairley, M., Ovigne, J.M., Sakaguchi, H., Schroeder, K., Tailhardat, M., Teissier, S., Winkler, P., 2011. Skin sensitisation: the Colipa strategy for developing and evaluating non-animal test methods for risk assessment. *Altex* **28**, 50–55.
- Moore, D.E., 1998. Mechanisms of photosensitization by phototoxic drugs. *Mutat. Res.* **422**, 165–173.
- Moore, D.E., 2002. Drug-induced cutaneous photosensitivity: incidence, mechanism, prevention and management. *Drug Saf.* **25**, 345–372.
- Nishi, K., Nishioka, H., 1982. Light induces mutagenicity of hair-dye p-phenylenediamine. *Mutat. Res.* **104**, 347–350.
- The Organisation for Economic Co-operation and Development (OECD), 2004. OECD Guideline for Testing of Chemicals, 432. *In vitro* 3T3 NRU Phototoxicity Test.
- Onoue, S., Hosoi, K., Wakuri, S., Iwase, Y., Yamamoto, T., Matsuoka, N., Nakamura, K., Toda, T., Takagi, H., Osaki, N., Matsumoto, Y., Kawakami, S., Seto, Y., Kato, M., Yamada, S., Ohno, Y., Kojima, H., 2013. Establishment and intra-/inter-laboratory validation of a standard protocol of reactive oxygen species assay for chemical photosafety evaluation. *J. Appl. Toxicol.* **33**, 1241–1250.
- Onoue, S., Igarashi, N., Yamada, S., Tsuda, Y., 2008a. High-throughput reactive oxygen species (ROS) assay: an enabling technology for screening the phototoxic potential of pharmaceutical substances. *J. Pharm. Biomed. Anal.* **46**, 187–193.
- Onoue, S., Kato, M., Yamada, S., 2012. Development of albuminous reactive oxygen species assay for photosafety evaluation under experimental biomimetic conditions. *J. Appl. Toxicol.*, in press, <http://dx.doi.org/10.1002/jat.2846>.
- Onoue, S., Kawamura, K., Igarashi, N., Zhou, Y., Fujikawa, M., Yamada, H., Tsuda, Y., Seto, Y., Yamada, S., 2008b. Reactive oxygen species assay-based risk assessment of drug-induced phototoxicity: classification criteria and application to drug candidates. *J. Pharm. Biomed. Anal.* **47**, 967–972.
- Onoue, S., Seto, Y., Gandy, G., Yamada, S., 2009. Drug-induced phototoxicity: an early *in vitro* identification of phototoxic potential of new drug entities in drug discovery and development. *Curr. Drug Saf.* **4**, 123–136.
- Onoue, S., Tsuda, Y., 2006. Analytical studies on the prediction of photosensitive/phototoxic potential of pharmaceutical substances. *Pharm. Res.* **23**, 156–164.
- Onoue, S., Yamauchi, Y., Kojima, T., Igarashi, N., Tsuda, Y., 2008c. Analytical studies on photochemical behavior of phototoxic substances: effect of detergent additives on singlet oxygen generation. *Pharm. Res.* **25**, 861–868.
- Scientific Committee on Cosmetic Products and Non-food products intended for Consumers (SCCNFP), 1999. Opinion of Concerning 2-Hydroxy-4-Methoxybenzophenone-5-Sulphonic Acid (Colipa n S40).

- Scientific Committee on Cosmetic Products and Non-food products intended for Consumers (SCCNFP), 2004. Evaluation and Opinion on Musk Xylene and Musk Ketone (SCCNFP/0817/04).
- Scientific Committee on Consumer Products (SCCP), 2006a. Opinion on methyl-N-methylantranilate (Photo-toxicity only) (SCCP/1068/06).
- Scientific Committee on Consumer Products (SCCP), 2006b. Opinion on phenylbenzimidazole sulfonic acid and its salts (SCCP/1056/06).
- Scientific Committee on Consumer Products (SCCP), 2008. Opinion on 4-methylbenzylidene camphor (SCCP/1184/08).
- Seto, Y., Hosoi, K., Takagi, H., Nakamura, K., Kojima, H., Yamada, S., Onoue, S., 2012. Exploratory and regulatory assessments on photosafety of new drug entities. *Curr. Drug. Saf.* 7, 140–148.
- Seto, Y., Kato, M., Yamada, S., Onoue, S., 2013. Development of micellar reactive oxygen species assay for photosafety evaluation of poorly water-soluble chemicals. *Toxicol. In Vitro* 27, 1838–1846.
- Spielmann, H., Liebsch, M., Döring, B., Moldenhauer, F., 1994. First results of an EC/COLIPA validation project of in vitro phototoxicity testing methods. *Altex* 11, 22–31.
- Tokura, Y., 1998. Quinolone photoallergy: photosensitivity dermatitis induced by systemic administration of photolabile drugs. *J. Dermatol. Sci.* 18, 1–10.
- Tokura, Y., 2009. Photoallergy. *Expert Rev. Dermatol.* 4, 263–270.
- Wan, L.S., Lee, P.F., 1974. CMC of polysorbates. *J. Pharm. Sci.* 63, 136–137.



Pirfenidone in respirable powder form for the treatment of pulmonary fibrosis: a safer alternative to the current oral delivery system?

“There is a need to develop efficacious strategies to avoid and/or reduce several systemic side effects, especially phototoxic responses, in order to improve clinical compliance and therapeutic outcome in the clinical treatment of IPF with pirfenidone.”

Keywords: idiopathic pulmonary fibrosis • phototoxicity • pirfenidone • respirable powder formulation

Idiopathic pulmonary fibrosis (IPF) is a progressive scarring disorder of the lungs with unknown aetiology and high mortality, characterized by dyspnea, cough, and ultimately respiratory failure [1]. The prevalence and incidence of IPF are estimated to be 14–42.7 and 6.8–16.3 per 100,000, respectively, and they increase markedly with aging [2]. Progressive deterioration of pulmonary function is inevitable, which increasingly limits the normal physical activity of the patients [3]. In the treatment of IPF, there are at least three clinical goals:

- Prevention or delay of disease progression using anti-fibrotic agents;
- Alleviation of symptoms;
- Management of disease-specific complications [4].

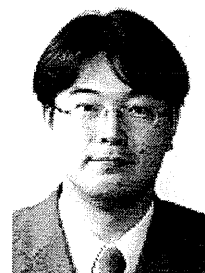
The increasing incidence and poor prognosis of IPF led to a marked acceleration in the discovery of new efficacious therapies in both industry and academia, with the therapeutic strategy against IPF shifting from corticosteroids to anti-fibrotic agents.

Pirfenidone [5-methyl-1-phenylpyridin-2-one], which exhibits good oral bioavailability, was developed as a novel anti-fibrotic and anti-inflammatory agent for suppressing the progression of lung, kidney and hepatic fibrosis and inflammatory events in experimental animal models [5–7]. The molecular mechanisms behind its anti-fibrotic activity have been reported, including regulation of key fibrotic cytokines and growth factors, inhibition of several inflammatory mediators, attenuation of fibroblast proliferation, differentiation, and related collagen synthesis, and restoration of

immune response balance [8]. These beneficial effects of pirfenidone could lead to treatments for fibrotic diseases, such as cardiac, renal, liver, and pulmonary fibrosis, and considerable efforts have been made towards conducting clinical trials that may help realize its therapeutic potential. In October 2008, pirfenidone, which is marketed by Shionogi & Co. (Osaka, Japan) under the trade name Pirespa[®], was approved as an orally available anti-fibrotic drug for the treatment of mild-to-moderate IPF [9].

Potential side-effects of orally dosed pirfenidone

Although pirfenidone has promising therapeutic potential for the treatment of IPF, orally taken pirfenidone often causes minor systemic side effects, such as nausea, anorexia, dizziness, rash, hepatic dysfunction, and phototoxicity [10–12]. Since pirfenidone is hepatically metabolized by CYP 1A2 and, to a lesser degree, by CYP2C9, CYP2C19, CYP2D6 and CYP2E1, patients with liver disease may suffer higher rates of side effects [12]. Oral administration of pirfenidone also causes hepatic injury with elevation of ALT or AST (typical biomarkers for hepatic injury) in a small proportion of patients, and thus, chronic use of pirfenidone at high dosages might cause hepatic injury, possibly leading to enhanced side effects. Gastrointestinal adverse events, related to pirfenidone treatment, include stomach discomfort and decreased appetite as representative symptoms. Administration of pirfenidone after meals has been demonstrated to reduce gastrointestinal side effects. The phototoxic skin response is a well-known adverse effect of pirfenidone treatment and its frequency has been demonstrated to be as much as approximately



Satomi Onoue

Author for correspondence:
Department of Pharmacokinetics & Pharmacodynamics, School of Pharmaceutical Sciences, University of Shizuoka, 52-1 Yada, Suruga-ku, Shizuoka 422-8526, Japan
Tel.: +81 54 264 5633
Fax: +81 54 264 5635
E-mail: onoue@u-shizuoka-ken.ac.jp



Shizuo Yamada

Department of Pharmacokinetics & Pharmacodynamics, School of Pharmaceutical Sciences, University of Shizuoka, 52-1 Yada, Suruga-ku, Shizuoka 422-8526, Japan

**FUTURE
SCIENCE**



50% in a clinical study [10]. In light of this, there is a need to develop efficacious strategies to avoid and/or reduce several systemic side effects, especially phototoxic responses, in order to improve clinical compliance and therapeutic outcome in the clinical treatment of IPF with pirfenidone.

“Most notably, RP formulation of pirfenidone, at a pharmacologically effective dose, could reduce the phototoxic potential of pirfenidone because of its lower systemic exposure and decreased distribution to light-exposed tissues relative to that caused by oral administration of pirfenidone at a phototoxic dose”

Phototoxicity of pirfenidone & its avoidance

As observed in pirfenidone medication, drug-induced phototoxicity is elicited by exposure of the skin and/or eyes to topical or systemic administration of pharmaceutical substances, followed by exposure to sunlight, especially UVA (320–400 nm) and UVB (290–320 nm) radiation [13]. Several classes of drug become reactive upon exposure to sunlight and cause phototoxic reactions, including photoirritation, photoallergy, and photogenotoxicity [14], and increasing attention has been drawn to drug-induced phototoxicity because of the gradual expansion of the UV portion in the solar spectrum. Although the phototoxicity of pirfenidone would be a major issue for clinical use, the molecular mechanisms for the phototoxicity have not been fully elucidated. In our previous study, pirfenidone was found to be photoreactive, and the generation of reactive oxygen species from photo-activated pirfenidone might lead to photoirritation of the skin, but not to photogenotoxic events [15]. Owing to possible reductions in medication compliance, drug-induced phototoxicity is one of the impediments in pharmaceutical development and a number of efforts have been made to avoid drug-induced phototoxic reactions. Theoretically, drug-induced phototoxicity is induced in light-exposed tissues, especially skin [13,16]. Therefore, controlling the skin exposure to pirfenidone and/or UV might be of great benefit to avoid, or attenuate, the phototoxic potential of pirfenidone. In the clinic, patients taking pirfenidone are usually advised to avoid exposure to sunlight with the use of photoprotective clothing and sunscreens. For the benefit of the

patients, marked reduction of pirfenidone dosage in oral administration would also be useful for attenuating pirfenidone-induced phototoxicity; however, there is a risk that this might offset its pharmacological effects. In this context, strategic development of well-suited drug delivery systems that target the lung might be efficacious for controlling phototoxic risk of pirfenidone, without attenuating its pharmacological effects.

Respirable powder formulation of pirfenidone

Several respirable formulation systems on small molecules and biologics have been developed for the treatment of airway inflammation, and inhalation therapy could achieve a high drug concentration in the lung with low systemic exposure [17,18]. These observations suggest that strategic application of pirfenidone as a respirable formulation system may lead to the successful development of efficacious pirfenidone medications with a wide safety margin. Trivedi and co-workers have reported on the development of biodegradable nanoparticles of pirfenidone using poly(lactide-*co*-glycolide) to achieve sustained release of pirfenidone [19]. Intratracheal administration of pirfenidone solution was found to demonstrate promise in ameliorating bleomycin-induced pulmonary fibrosis in mice, and pulmonary delivery of nanoparticle suspension was more effective with dosing once a week. The respirable liquid formulation of pirfenidone with sustained releasing-property might be promising for treatment of IPF; however, on the basis of the poor photostability of pirfenidone in the solution state [20], a nebulizer system using the liquid formulation of pirfenidone may not be suitable for inhalation therapy. This could be a rationale for the development of a pirfenidone-loaded respirable powder (RP) formulation. In a previous study, we developed a RP formulation of pirfenidone using a jet milling system with the aim of improving photosafety and reducing nominal dose. According to our results from the photostability testing, the RP formulation of pirfenidone, as well as pirfenidone powder, was more highly photostable than that in the solution state. The RP formulation of pirfenidone exhibited reasonable inhalation performance, such as fine dispersibility and suitable particle size distribution for inhalation therapy. In the experimental asthma/chronic obstructive pulmonary disease model rats, the inhaled RP formulation of pirfenidone was found to attenuate inflammatory symptoms and severe neutrophilia in the

pulmonary tissue. Most notably, RP formulation of pirfenidone, at a pharmacologically effective dose, could reduce the phototoxic potential of pirfenidone because of its lower systemic exposure and decreased distribution to light-exposed tissues relative to that caused by oral administration of pirfenidone at a phototoxic dose [20]. According to the pharmacokinetic data, RP formulation of pirfenidone would also be advantageous for avoidance of other systemic side effects, thus, the newly developed RP system may provide efficacious and safe medication for the clinical treatment of IPF as an interesting alternative to oral therapy with a better safety margin.

Future perspective

Currently, pirfenidone provides an appropriate option as first-line therapy and a significant treatment benefit for patients with IPF, whereas pirfenidone medication at high dose sometimes causes phototoxicity and other systemic side effects. Strategic delivery of pirfenidone to the pulmonary tissue would offer two primary

benefits: reduced nominal dose, and reduced off-target drug exposure, possibly leading to lower cost of goods and reducing systemic side effects. However, the local and systemic safety of RP system upon chronic use is still uncertain; therefore, further safety assessments would be needed before its clinical use. In addition, there might be medical needs for implementation of new drug-delivery system concepts for longer-duration of action, possibly leading to further improvements on dosing frequency and therapeutic compliance in clinical treatment of IPF with pirfenidone.

Financial & competing interests disclosure

The authors have no relevant affiliations or financial involvement with any organization or entity with a financial interest in or financial conflict with the subject matter or materials discussed in the manuscript. This includes employment, consultancies, honoraria, stock ownership or options, expert testimony, grants or patents received or pending, or royalties.

No writing assistance was utilized in the production of this manuscript.

References

- King TE Jr, Pardo A, Selman M. Idiopathic pulmonary fibrosis. *Lancet* 378(9807), 1949–1961 (2011).
- Navaratnam V, Fleming KM, West J *et al.* The rising incidence of idiopathic pulmonary fibrosis in the U.K. *Thorax* 66(6), 462–467 (2011).
- Cottin V. Changing the idiopathic pulmonary fibrosis treatment approach and improving patient outcomes. *Eur. Respir. Rev.* 21(124), 161–167 (2012).
- Adamali HI, Maher TM. Current and novel drug therapies for idiopathic pulmonary fibrosis. *Drug Des. Devel. Ther.* 6, 261–272 (2012).
- Iyer SN, Gurujeyalakshmi G, Giri SN. Effects of pirfenidone on transforming growth factor-beta gene expression at the transcriptional level in bleomycin hamster model of lung fibrosis. *J. Pharmacol. Exp. Ther.* 291(1), 367–373 (1999).
- Lasky J. Pirfenidone. *IDrugs* 7(2), 166–172 (2004).
- Schaefer CJ, Ruhmundt DW, Pan L, Seiwert SD, Kossen K. Antifibrotic activities of pirfenidone in animal models. *Eur. Respir. Rev.* 20(120), 85–97 (2011).
- Macias-Barragan J, Sandoval-Rodriguez A, Navarro-Partida J, Armendariz-Borunda J. The multifaceted role of pirfenidone and its novel targets. *Fibrogenesis Tissue Repair* 3, 16 (2010).
- Richeldi L, Yasothan U, Kirkpatrick P. Pirfenidone. *Nat. Rev. Drug Discov.* 10(7), 489–490 (2011).
- Taniguchi H, Ebina M, Kondoh Y *et al.* Pirfenidone in idiopathic pulmonary fibrosis. *Eur. Respir. J.* 35(4), 821–829 (2010).
- Hilberg O, Simonsen U, Du Bois R, Bendstrup E. Pirfenidone: significant treatment effects in idiopathic pulmonary fibrosis. *Clin. Respir. J.* 6(3), 131–143 (2012).
- Carter NJ. Pirfenidone: in idiopathic pulmonary fibrosis. *Drugs* 71(13), 1721–1732 (2011).
- Onoue S, Seto Y, Gandy G, Yamada S. Drug-induced phototoxicity: an early *in vitro* identification of phototoxic potential of new drug entities in drug discovery and development. *Curr. Drug Saf.* 4(2), 123–136 (2009).
- Epstein JH, Wintroub BU. Photosensitivity due to drugs. *Drugs* 30(1), 42–57 (1985).
- Seto Y, Inoue R, Kato M, Yamada S, Onoue S. Photosafety assessments on pirfenidone: photochemical, photobiological, and pharmacokinetic characterization. *J. Photochem. Photobiol. B.* 120, 44–51 (2013).
- Seto Y, Inoue R, Ochi M, Gandy G, Yamada S, Onoue S. Combined use of *in vitro* phototoxic assessments and cassette dosing pharmacokinetic study for phototoxicity characterization of fluoroquinolones. *AAPS J.* 13(3), 482–492 (2011).
- Onoue S, Aoki Y, Kawabata Y *et al.* Development of inhalable nanocrystalline solid dispersion of tranilast for airway inflammatory diseases. *J. Pharm. Sci.* 100(2), 622–633 (2011).
- Onoue S, Sato H, Kawabata Y, Mizumoto T, Hashimoto N, Yamada S. *In vitro* and *in vivo* characterization on amorphous solid dispersion of cyclosporine A for inhalation therapy. *J. Control. Release* 138, 16–23 (2009).
- Trivedi R, Redente EF, Thakur A, Riches DW, Kompella UB. Local delivery of biodegradable pirfenidone nanoparticles ameliorates bleomycin-induced pulmonary fibrosis in mice. *Nanotechnology* 23(50), 505101 (2012).
- Onoue S, Seto Y, Kato M, Aoki Y, Kojo Y, Yamada S. Inhalable powder formulation of pirfenidone with reduced phototoxic risk for treatment of pulmonary fibrosis. *Pharm. Res.* 30(6), 1586–1596 (2013).

Development of an albuminous reactive oxygen species assay for photosafety evaluation under experimental biomimetic conditions

Satomi Onoue*, Masashi Kato and Shizuo Yamada

ABSTRACT: The generation of reactive oxygen species (ROS) from an ultraviolet (UV)-exposed chemical can be an experimental indicator of phototoxic potential. The aim of the present study was to develop a new ROS assay using serum albumin to provide photosafety assessment under experimental biomimetic conditions. To assess assay robustness, a validation study on an albuminous ROS (aROS) assay was conducted with a focus on intra- and inter-day precisions and Z'-factor reflecting both the assay signal-to-noise ratio and variation associated with signal measurements. In the aROS assay on quinine HCl (200 μ M), a typical phototoxic drug, both intra- and inter-day precisions (coefficient of variation; CV) were found to be below 4%, and the Z'-factors for singlet oxygen and superoxide suggested a large separation band between samples and blank signals. To evaluate the prediction capacity, the aROS and ROS assays were applied to 21 phototoxins and 10 non-phototoxic chemicals. Upon aROS assay on these model chemicals, the individual specificity was 100%, and the positive and negative predictivities were found to be 100% and 81.8%, respectively. The aROS assay can be employed for poorly soluble chemicals for which the ROS assay is unavailable. Comparing the ROS assay data, there seemed to be a photochemical transition of some chemicals in albuminous solution. A molecular interaction between albumin and chemical was also assessed by UV and fluorescent spectroscopic analyses, and the results suggested the limited relationship between the albumin-chemical interaction and the photochemical change. The aROS assay may allow photosafety assessment of new drug entities with a wide range of applicability partly under experimental biomimetic conditions. Copyright © 2013 John Wiley & Sons, Ltd.

Keywords: albumin; photoreactivity; photosafety assessment; phototoxicity; reactive oxygen species

Introduction

Phototoxic skin responses can be caused by the combined effects of external phototoxic drugs and sunlight irradiation, consisting of partial ultraviolet (UV) B, UVA and visible (VIS) lights (Stein and Scheinfeld, 2007); the side effects could lead to reductions in medication compliance. There are at least three types of phototoxic reaction, including photoirritation, photogenotoxicity and photoallergy, with different mechanisms and pathologic features (Moore, 2002). To date, in order to avoid these drug-induced phototoxic reactions, considerable efforts have been made, which include the clinical use of a sunscreen (Dubakiene and Kupriene, 2006), the development of a new formulation for controlling the skin distribution of drugs (Seto *et al.*, 2011a) and, most notably, early identification of a phototoxic potential for new drug entities (Onoue *et al.*, 2009). Strategic screening for photosafety is necessary at the early phase of the drug discovery process and even before introducing drugs into clinical therapy, as rapid and reliable photosafety evaluation would be of great help for the prevention of unwanted drug reactions in humans. Therefore, a number of assay systems have been designed for the assessment of photosensitive/phototoxic potential through analytical and biochemical methods (Onoue *et al.*, 2009; Seto *et al.*, 2012).

According to the first law of photochemistry, the primary event in any photochemical and/or photobiochemical process is the absorption of photon energy, followed by the generation

of reactive oxygen species (ROS). From a theoretical standpoint, the ROS assay was developed for *in vitro* photoreactivity and phototoxicity assessment, in which the generation of singlet oxygen and superoxide anion from photo-activated chemicals is quantitatively determined (Onoue and Tsuda, 2006; Onoue *et al.*, 2008a). The good relationship between ROS data and *in vivo* phototoxicity revealed the prediction capacity of the ROS assay; however, through multi-laboratory validation study, there appeared to be two assay limitations, namely (i) false-positive predictions and (ii) solubility issues (Onoue *et al.*, 2012). The ROS assay is commonly used for early photosafety evaluation with appropriate follow-up assessments, so the former issue may not always be problematic as long as chemicals are not falsely predicted as non-phototoxic. In contrast, experimental problems arising from the limited solubility have a major impact on assay performance and applicability. In such cases, appropriate options to modify the ROS assay system would be required for reliable photosafety assessment on poorly water-soluble chemicals.

*Correspondence to: Satomi Onoue, Department of Pharmacokinetics and Pharmacodynamics, School of Pharmaceutical Sciences, University of Shizuoka, 52-1 Yada, Suruga-ku, Shizuoka 422-8526, Japan. E-mail: onoue@u-shizuoka-ken.ac.jp

Department of Pharmacokinetics and Pharmacodynamics, School of Pharmaceutical Sciences, University of Shizuoka, 52-1 Yada, Suruga-ku, Shizuoka 422-8526, Japan

In the present study, to overcome these limitations, a modified ROS assay system was newly developed using bovine serum albumin (BSA) for two major reasons: (i) co-existing albumin might provide an experimental biomimetic environment to some extent as some chemicals tend to interact with albumin, and (ii) albumin could also act as a potent solubilizer for poorly water-soluble drugs (Kurono *et al.*, 1987). Determination of ROS in an albuminous solution might partly reflect the photochemical behavior of photosensitizers *in vivo*, and the albuminous ROS (aROS) assay system might be more effective for photosafety evaluation with fewer false predictions. In this study, 21 phototoxins and 10 non-phototoxic chemicals were assessed by both ROS and aROS assays to clarify the prediction capacity of these assay systems. The precision of the aROS assay was also assessed by repeated measurement and calculation of the Z'-factor, a characteristic parameter reflecting the quality of the assay. In addition, spectroscopic experiments were carried out to evaluate the possible interaction of photosensitizing compounds with albumin by UV and fluorescent spectrometry.

Materials and Methods

Chemicals

According to the reported *in vitro/in vivo* photosafety information and clinical observations (Alvarez-Fernandez *et al.*, 2000; Lim and Hawk, 2008; Onoue *et al.*, 2012; Quintero and Miranda, 2000; Selvaag, 1997; Seto *et al.*, 2011b), 2 standard chemicals and 29 test chemicals, including 20 phototoxins and 9 non-phototoxic drugs/chemicals, were selected as model chemicals for the present study (Table 1).

Quinine HCl (1), chlorpromazine HCl (6), glibenclamide (8), gliclazide (9), glimepiride (10), griseofulvin (11), norfloxacin (16), ofloxacin (17), piroxicam (18), promethazine HCl (19), quinidine H₂SO₄ 2H₂O (20), aspirin (23), benzocaine (24), erythromycin (25), *para*-aminobenzoic acid (PABA, 27), penicillin G (28), phenytoin (29), sodium dodecyl sulfate (SDS, 30), warfarin Na (31), Na₂HPO₄ 2H₂O, Na₂HPO₄ 12H₂O, dimethyl sulfoxide (DMSO), *p*-nitrosodimethylaniline, imidazole and nitroblue tetrazolium (NBT) were obtained from

Table 1. Outcomes from reactive oxygen species (ROS) and albuminous reactive oxygen species (aROS) assays on known phototoxins and non-phototoxic chemicals

No.	Chemical name	CAS No.	Form	Singlet oxygen ($\Delta A_{440\text{nm}} \cdot 10^3$)		Superoxide ($\Delta A_{560\text{nm}} \cdot 10^3$)		Photosafety information	
				ROS assay	aROS assay	ROS assay	aROS assay	Phototoxicity	Photoallergy
Positive/Negative controls									
1	Quinine HCl	6119-47-7	Solid	519±8	455±7	398±3	617±7	+ a	
2	Sulisobenzone	4065-45-6	Solid	-1±1	-70±5	-19±1	4±35	- a	
Phototoxic chemicals									
3	6-Methylcoumarin	92-48-8	Solid	148±34	126±11	108±15	12±2	+ a	+ b
4	Bithionol	97-18-7	Solid	39±9	-3±14	14±2	43±9	+ a	+ b
5	Chlorhexidine	55-56-1	Solid	-5±0	-27±3	23±1	49±2	+ a	+ b
6	Chlorpromazine HCl	69-09-0	Solid	-11±12	48±20	63±9	65±2	+ a	+ b
7	Diclofenac Na	15307-79-6	Solid	311±2	80±30	403±14	-13±1	+ a	+ b
8	Glibenclamide	10238-21-8	Solid	5±12	35±6	12±7	57±0	+ d	
9	Gliclazide	21187-98-4	Solid	-1±4	-70±5	225±3	165±7	+ d	
10	Glimepiride	93479-97-1	Solid	-13±4	0±3	41±13	38±1	+ c	
11	Griseofulvin	126-07-8	Solid	22±10	-18±5	27±6	-2±2	+ a	+ b
12	Hexachlorophene	70-30-4	Solid	266±4	-10±8	-25±15	10±6	+ a	+ b
13	Itraconazole	84625-61-6	Solid	86±4	35±4	-11±9	28±1	+ c	+ c
14	Ketoprofen	22071-15-4	Solid	301±8	336±16	112±7	66±1	+ a	+ b
15	Lomefloxacin HCl	98079-52-8	Solid	603±3	355±15	82±6	36±4	+ f	+ b
16	Norfloxacin	70458-96-7	Solid	179±18	238±17	100±2	41±2	+ a	+ b
17	Ofloxacin	82419-36-1	Solid	169±15	328±21	416±14	524±23	+ d	+ b
18	Piroxicam	36322-90-4	Solid	166±11	358±3	103±6	456±10	+ a	+ b
19	Promethazine HCl	58-33-3	Solid	73±4	175±34	56±3	93±4	+ a	+ b
20	Quinidine H ₂ SO ₄ 2H ₂ O	6591-63-5	Solid	592±26	408±4	405±19	555±2	+ a	+ b
21	Tetracycline	60-54-8	Solid	221±12	105±8	200±2	211±4	+ a	+ b
22	Tolbutamide	64-77-7	Solid	-9±13	3±6	44±6	50±3	+ d	
Non-phototoxic chemicals									
23	Aspirin	50-78-2	Solid	4±12	-2±45	25±26	-13±8	- a	
24	Benzocaine	94-09-7	Solid	-9±6	-88±3	3±16	-7±16	- a	
25	Erythromycin	114-07-8	Solid	-29±10	-12±8	6±5	-4±2	- a	
26	Octyl methoxycinnamate	5466-77-3	Solid	11±9	-52±3	-11±11	17±2	- a	
27	PABA	150-13-0	Solid	-17±16	-17±17	-16±10	-5±10	- a	
28	Penicillin G	113-98-4	Solid	14±9	3±19	46±22	-6±1	- a	
29	Phenytoin	57-41-0	Solid	-28±23	-13±33	17±26	-8±4	- a	
30	SDS	151-21-3	Solid	7±4	17±20	3±2	-14±8	- a	
31	Warfarin Na	129-06-6	Solid	7±1	-69±25	55±1	-19±10	- a	

ROS and aROS assays were basically carried out for test chemicals at a concentration of 200 μM , and data on the diluted chemicals are boxed (100 μM) or emphasized with gray (50 μM) and black (20 μM). References: a, (Onoue *et al.*, 2012); b, (Lim and Hawk, 2008); c, (Selvaag, 1997); d, (Quintero & Miranda, 2000); and e, (Seto *et al.*, 2011b).

Table 2. Intra- and inter-day (days 1 and 3) precision for reactive oxygen species (ROS) of irradiated quinine HCl (200 μ M) in the presence of bovine serum albumin (BSA)

	Generation of reactive oxygen species, mean \pm SD (%RSD)	
	Singlet oxygen (Decrease of $A_{440\text{ nm}} \times 10^3$)	Superoxide (Increase of $A_{560\text{ nm}} \times 10^3$)
Intra-day	435 \pm 10.6 (2.4)	576 \pm 21.6 (3.8)
Inter-day	436 \pm 9.1 (2.1)	592 \pm 7.6 (1.3)

Data represent mean \pm standard deviation (SD) of 5 experiments for intra-day precision and 10 experiments for inter-day precision.

Wako Pure Chemical Industries (Osaka, Japan). Sulisobenzone (**2**), bithionol (**4**), hexachlorophene (**12**), ketoprofen (**14**) and octyl methoxycinnamate (**26**) were purchased from Tokyo Chemical Industry (Tokyo, Japan). 6-Methylcoumarin (**3**), chlorhexidine (**5**), diclofenac Na (**7**), lomefloxacin HCl (**15**), tetracycline (**21**), tolbutamide (**22**) and bovine serum albumin (BSA) were purchased from Sigma-Aldrich Japan (Tokyo, Japan). Itraconazole (**13**) was bought from LKT Laboratories (St. Paul, MN, USA). A quartz reaction container for a high-throughput ROS assay (Onoue et al., 2008a) was constructed by Ozawa Science (Aichi, Japan).

Irradiation

The ROS and aROS assays were conducted using Atlas Suntest CPS plus (Atlas Material Technology LLC, Chicago, USA) equipped with a xenon arc lamp (1500 W). A UV special filter was installed to adapt the spectrum of the artificial light source to that of natural daylight, and the Atlas Suntest CPS series had a high irradiance capability that met CIE85/1989 daylight simulation requirements. The irradiation test was carried out at 25 °C with an irradiance of c. 2.0 mW/cm² as determined by the calibrated UVA detector Dr Hönle no. 0037 (Dr Hönle, München, Germany).

ROS Assay Procedure

The ROS assay was designed to detect both singlet oxygen and superoxide generated from photo-irradiated chemicals (Onoue et al., 2008a, 2008b). Briefly, singlet oxygen was measured in an aqueous solution by spectrophotometrically monitoring the bleaching of *p*-nitrosodimethylaniline at 440 nm using imidazole as a selective acceptor of singlet oxygen. Samples, containing the tested chemical (20–200 μ M), *p*-nitrosodimethylaniline (50 μ M), and imidazole (50 μ M) in 20 mM sodium phosphate buffer (NaPB, pH 7.4), were mixed in a tube. For the aROS assay, BSA at a concentration equal to that of the tested chemical was added to the reaction mixture. Two hundred microliters of the sample was transferred into a well of a plastic 96-well plate (clear, untreated, flat-bottomed; Asahi Glass Co., Ltd., Tokyo, Japan) and checked for precipitation before light exposure. The plate was subjected to measurement of absorbance at 440 nm using a SAFIRE microplate spectrophotometer (TECAN, Männedorf, Switzerland). The plate was fixed in the quartz reaction container with a quartz cover, and then irradiated with the simulated sunlight for 1 h. After agitation on a plate shaker,

the UV absorbance at 440 nm was measured. For the determination of superoxide, samples containing the tested chemical (20–200 μ M), NBT (50 μ M), and/or BSA (20–200 μ M) in 20 mM NaPB were irradiated with the simulated sunlight for 1 h, and the reduction in NBT was measured by the increase in absorbance at 560 nm in the same manner as the singlet oxygen determination. Experiments were performed in triplicate wells in three independent runs. As the final concentration, 200 μ M of the test chemical solutions should have been subjected to the ROS assay. However, when precipitation could be observed at 200 μ M under an optical microscope, additional experiments were performed at 20, 50, or 100 μ M. When precipitation was observed at 20 μ M in the reaction mixture, no further experiment was carried out.

Criteria for Data Acceptance and Judgment

According to the result (mean of triplicate determinations) from the ROS assay, photoreactivity on each test chemical should be judged to be (i) positive with singlet oxygen ($\Delta A_{440\text{ nm}} \times 10^3$): 25 or more; and/or superoxide ($\Delta A_{560\text{ nm}} \times 10^3$): 20 or more, or (ii) negative with singlet oxygen: less than 25 ($\Delta A_{440\text{ nm}} \times 10^3$) and superoxide ($\Delta A_{560\text{ nm}} \times 10^3$): less than 20. The final decision should be made as follows: (i) positive: above the threshold level for singlet oxygen or superoxide; or (ii) negative: below the threshold level for both singlet oxygen and superoxide.

These criteria were defined for the ROS assay on tested chemicals at a concentration of 200 μ M, and, therefore, they would not be theoretically applicable to the outcomes from assays at a lower concentration (< 200 μ M). However, the tested chemicals could be identified to be phototoxic as long as the ROS data at a lower concentration (< 200 μ M) surpassed these tentative classification criteria, so that these criteria might still be available for a positive prediction on the diluted samples. In contrast, it would be challenging to make negative predictions on the basis of a ROS assay under dilution.

Z'-factor

To evaluate the robustness of the aROS assay, the Z'-factor, a statistical function, was calculated using the following equation: $Z' = 1 - (3\sigma_{c+} + 3\sigma_{c-}) / |\mu_{c+} - \mu_{c-}|$ (Zhang et al., 1999). The means of the positive and negative control signals are denoted as μ_{c+} and μ_{c-} , respectively. The SDs of the signals are denoted as σ_{c+} and σ_{c-} , respectively. The difference between the means, $|\mu_{c+} - \mu_{c-}|$, defines the assay dynamic range.

Solubility Test

Equilibrium solubility of glibenclamide (**8**) was measured as follows: an excessive amount of glibenclamide (**8**) was added to the reaction mixture for superoxide with or without 200 μM of BSA to keep the concentration constant at 1 mg ml^{-1} . Samples were put in a shaker and shaken for 48 h at 25 °C. The samples were centrifuged at 15 000 g for 5 min, and the supernatant was mixed with a threefold volume of acetonitrile and then centrifuged at 10 000 g for 5 min. The concentration of dissolved glibenclamide (**8**) in the supernatant was determined by Waters Acquity UPLC system (Waters, Milford, MA, USA), which included a binary solvent manager, sample manager, column compartment and a SQD connected with MassLynx software. An Acquity UPLC BEH C 18 column (particle size: 1.7 μm , column size: 2.1 \times 50 mm; Waters) was used, and column temperature was maintained at 40 °C. Samples were separated using a gradient mobile phase consisting of acetonitrile (A) and 0.1% formic acid (B) with a flow rate of 0.25 ml min^{-1} , and the retention time of glibenclamide (**8**) was 2.4 min. The gradient condition of the mobile phase was 0–1.0 min, 50% A; 1.0–4.0 min, 50–95% A; and 4.0–5.0 min, 95% A. Analysis was carried out using selected ion recording (SIR) for specific m/z 495 for glibenclamide (**8**) [$M + H$]⁺.

UV Spectral Analysis

Chemicals were dissolved in 20 mM sodium phosphate buffer (NaPB, pH 7.4) at a final concentration of 20 μM . UV/VIS absorption spectra were recorded with a Hitachi U-2010 spectrophotometer (Hitachi High-Technologies Corporation, Tokyo, Japan) interfaced to a PC for data processing (software: Spectra Manager). A spectrofluorimeter quartz cell with 10-mm path length was employed.

Fluorescence Quenching Assay

To ensure a molecular interaction between serum albumin and the tested chemical, a fluorescence quenching assay was carried out according to a previous report with some modifications (Fukuohara *et al.*, 2012). Each tested chemical and/or BSA were dissolved in 20 mM NaPB (pH 7.4) at a final concentration of 2 μM . After incubation at 25 °C for 30 min, the intrinsic tryptophan fluorescence in BSA solution with or without tested chemical was measured using a SAFIRE microplate spectrophotometer (TECAN) with an excitation wavelength of 295 nm and an emission wavelength of 340 nm.

Results and Discussion

ROS Generation from Quinine HCl with or without BSA

Serum albumin is the most abundant protein in plasma, accounting for c. 60% of its total protein content and providing c. 80% of the blood osmotic pressure (Carter and Ho, 1994). Considerable attention has also been drawn to the biological functions of serum albumin for drug transport and storage in vertebrates through the formation of non-covalent binding. Therefore, even although the condition in the presence of albumin might not be accurately biomimetic, serum albumin has been widely used to provide experimental biomimetic conditions in assay development (Andrade and Costa, 2008; Danel *et al.*, 2006).

The interaction of albumin with a poorly water-soluble chemical also led to an improvement in its solubility; therefore, the use of albumin for the ROS assay would offer biomimetic experimental conditions partly and solubility enhancement. To verify the feasibility of the aROS assay, ROS and aROS assays were carried out for two standard chemicals, quinine HCl (**1**), a typical phototoxin (Moore, 2002), and sulisobenzone (**2**), a non-phototoxic chemical (Portes *et al.*, 2002). In the ROS assay (Table 1), quinine HCl (**1**: 200 μM) generated both singlet oxygen and superoxide when exposed to the simulated sunlight (c. 2.0 mW/cm^2) for 1 h, whereas ROS generation was negligible from irradiated sulisobenzone (**2**: 200 μM). Both standards did not exhibit any ROS generation under light protection (data not shown). Similar photochemical responses on these standards were also observed in the aROS assay, whereas the addition of equimolar albumin into quinine HCl (**1**: 200 μM) resulted in transition of the generated ROS, as evidenced by c. 12% decrease in singlet oxygen and c. 55% increase in superoxide. These findings were partly in agreement with a previous observation, showing that non-covalently bound serum albumin modulated the photochemical behavior of a bacteriochlorophyll derivative (Ashur *et al.*, 2009). It would be highly challenging to mimic the physiological environment exactly; however, aROS data on quinine HCl (**1**) might partly reflect the *in vivo* photochemical behavior upon interaction with serum albumin.

To assess the robustness and reproducibility of the aROS assay, the Z'-factor was also calculated according to the method of Zhang *et al.* (1999). The Z'-factor is designed to reflect both the assay signal noise ratio and the variation associated with the signal measurements. Hence, the Z'-factor is commonly utilized for quality assessment in assay development and optimization, as well as evaluation of the reproducibility of assays used for high-throughput screening campaigns (Rega *et al.*, 2007). The Z'-factor is close to 1.0 in an ideal assay, and a Z'-factor greater than 0.5 is indicative of an excellent assay, whereas assays with Z' values less than 0.5 show a small separation band. Typical values from multiple measurements (21 times) of quinine HCl (**1**: 200 μM) and sulisobenzone (**2**: 200 μM) are shown in Fig. 1A (singlet oxygen) and 1B (superoxide). The Z'-factors for the determination of singlet oxygen and superoxide were calculated to be 0.93 and 0.79, respectively, demonstrating that the assay allows a large separation band between samples and blank signals and thereby confirming its suitability for high-throughput screening. The overall precision of the aROS assay was also evaluated by analyzing nine samples of quinine HCl (**1**) solution at 200 μM (Table 2). The intra-day coefficients of variation (CV) for the detection of singlet oxygen and superoxide generated from irradiated quinine HCl (**1**) were found to be 2.4% and 3.8%, respectively. In addition, the inter-day CV values for quinine HCl (**1**) were calculated to be 2.1% for singlet oxygen and 1.3% for superoxide. Thus, the CV value obtained was below 4%, showing that the proposed analytical method has good intra- and inter-day precision.

Prediction Capacity of Albuminous ROS Assay

To evaluate the predictive capacity of an aROS assay, in addition to 2 standard chemicals (**1** and **2**), 29 chemicals, consisting of 20 known phototoxins (**3–22**) and 9 non-phototoxic drugs/chemicals (**23–31**), were also assessed by the ROS and aROS assays (Table 1 and Fig. 2).

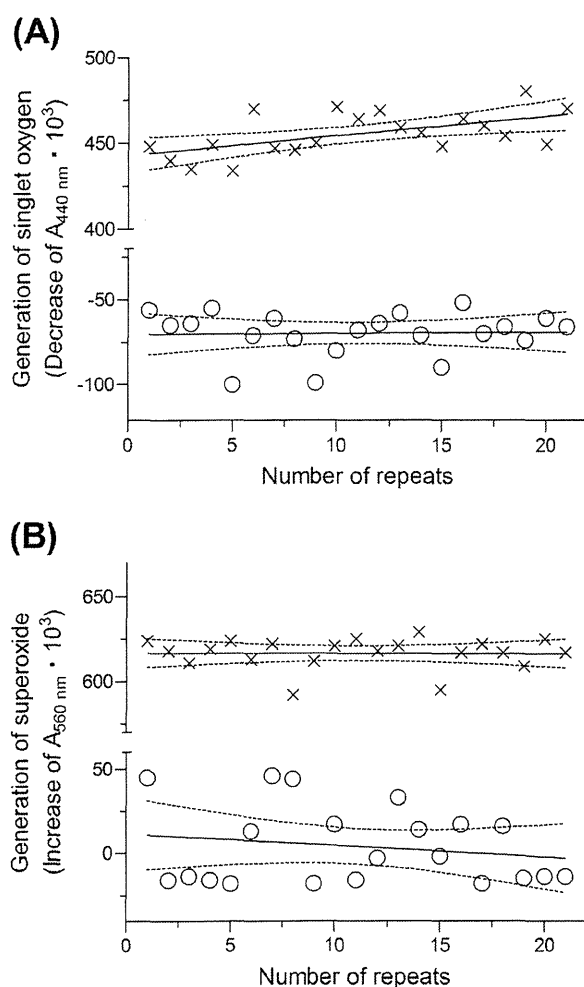


Figure 1. Representative multiple measurement data used to calculate the Z'-factor for the albuminous reactive oxygen species (aROM) assay. Quinine HCl as a positive control (x) or sulisobenzone as a negative control (o) at a concentration of 200 μM was dissolved in 20 mM sodium phosphate buffer (pH7.4) and exposed to simulated sunlight (2.0 mW/cm²) for 60 min. Generation of (A) singlet oxygen and (B) superoxide was determined. Lines indicate mean ± 95% confidence interval.

For the ROS assay, 26 chemicals (84% of the total) could be assessed at the concentration of 200 μM, and 5 chemicals had to be diluted to a final concentration of 20, 50 or 100 μM because of limited solubility in aqueous media. Most phototoxins even under dilution demonstrated potent ability to generate singlet oxygen, superoxide, or both under UV/VIS exposure (Fig. 2A). In contrast, ROS generation from most non-phototoxic chemicals was negligible, except for aspirin (23), penicillin G (28) and warfarin Na (31). According to the threshold values [25 for singlet oxygen ($\Delta A_{440\text{ nm}} \times 10^3$) and 20 for superoxide anion ($\Delta A_{560\text{ nm}} \times 10^3$)] defined for the ROS data at 200 μM, most phototoxins tested here were correctly identified to be phototoxic by the ROS assay, whereas only glibenclamide (8) was unevaluable because of its poor solubility. Of all 10 non-phototoxic chemicals, 5 compounds (2, 24, 25, 27 and 29) were found to be non-phototoxic on the basis of ROS data at 200 μM, and the negativity for 2 chemicals (26 and 30) could not be fully proven as they were assessed at a lower concentration. Thus, some

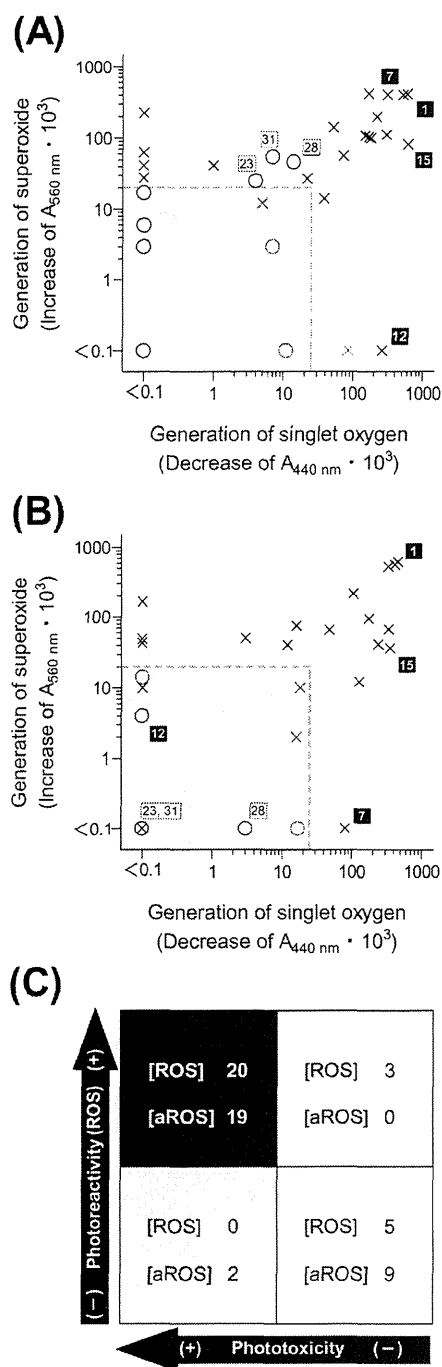


Figure 2. Predictive capacity of the albuminous reactive oxygen species (aROS) assay. Plot of singlet oxygen data versus superoxide data for all tested chemicals obtained from the ROS assay (A) and aROS assay (B). ○, non-phototoxic chemicals; and ×, phototoxins at concentrations of 20–100 (red symbols) and 200 μM (black symbols). Symbols with a number represent the data on quinine HCl (1), diclofenac Na (7), hexachlorophene (12), lomefloxacin HCl (15), aspirin (23), penicillin G (28) and warfarin Na (31). Each value represents the mean of three experiments. According to the criteria for phototoxins (200 μM) defined previously, the shaded region is indicative of low phototoxic potential. (C) Positive and negative predictivity of the ROS and aROS assays as compared with the *in vitro/in vivo* phototoxicity.

chemicals were unevaluable by the ROS assay because of their limited solubility, and 3 non-phototoxic chemicals (**23**, **28** and **31**) were falsely identified as phototoxic and/or photosensitive (Fig. 2C).

With respect to the aROS assay, only 2 chemicals (**13** and **26**) had to be diluted for photosafety evaluation, and c. 94% of tested chemicals could be successfully assessed at 200 μM (Fig. 2B). In the aROS assay, most tested chemicals exhibited a similar photochemical behavior to that observed in the ROS assay. Although reliable photosafety evaluation of glibenclamide (**8**) could not be achieved by the ROS assay owing to the limited solubility, the aROS assay provided consistent prediction results. The solubility of glibenclamide (**8**) in ROS assay buffer, containing *p*-nitrosodimethylaniline (50 μM), and imidazole (50 μM) in 20 mM NaPB (pH 7.4), was determined to be 114 μM (56.3 $\mu\text{g ml}^{-1}$), whereas that in aROS assay buffer was increased to 215 μM (106.2 $\mu\text{g ml}^{-1}$). The expansion of the applicability domain should be attributable to the solubilizing function of co-existing BSA at an equimolar concentration. Most notably, transition in photochemical properties was observed for some non-phototoxic chemicals such as aspirin (**23**), penicillin G (**28**) and warfarin Na (**31**) in the presence of BSA, and they were then correctly predicted as non-phototoxic by the aROS assay. There also appeared to be a photochemical transition in two phototoxins (**11** and **12**), and the aROS assay demonstrated that these phototoxins were falsely deduced to be less phototoxic. In the present study, the photochemical behavior of tested chemicals could vary in the presence of serum albumin, possibly affecting the prediction capacity in photosafety assessment. With respect to hexachlorophene (**12**), this agent has been reported to cause photocontact dermatitis when applied topically in humans; however, hexachlorophene (**12**) was identified to be non-phototoxic in both *in vitro* 3T3 NRU phototoxicity testing (Jones and King, 2003) and *in vivo* animal experiments (Spielmann *et al.*, 1998). Thus, *in vivo* and *in vitro* phototoxicity of hexachlorophene (**12**) is a matter of controversy, and it is still doubtful whether the reasonable photosafety assessment of hexachlorophene (**12**) can be achieved by ROS and/or an aROS assay. There is also no denying that the photosensitivity of hexachlorophene (**12**) might be attenuated through interaction with serum albumin when applied orally.

The prediction capacity of the ROS and aROS assays is summarized in Fig. 2C. The individual specificities for ROS and aROS assays were 62.5% and 100%, respectively. The positive and negative predictivities for ROS and aROS assays were found to be 87.0/100% (ROS assay) and 100/81.8% (aROS assay). Thus, unlike the ROS assay, the aROS assay provided no false positives, but two false negatives instead.

The aROS assay might be superior to the ROS assay in terms of the wide applicability domain as well, and such a high prediction capacity may indicate its potential as a reliable photosafety assessment tool. The aROS assay may be efficacious for early hazard identification in photosafety assessment; however, a thorough understanding of the assay limitations should be obtained to avoid overestimation and misleading conclusions in exploratory and regulatory use.

Spectroscopic Analysis of the Interaction between Phototoxin and Albumin

In light of the photochemical transition of some chemicals in the presence of BSA, further studies were carried out to clarify

the possible relationship between molecular interaction and photochemical change in more detail. To evaluate the interaction between serum albumin and chemical, UV spectral patterns of two standards (**1** and **2**) and the tested chemicals with high photochemical transitions were measured in the presence and absence of BSA; these included diclofenac Na (**7**), hexachlorophene (**12**), lomefloxacin HCl (**15**) and warfarin Na (**31**) (Fig. 3). As radiation below 300 nm in sunlight hardly reaches the surface of the earth owing to effective absorption by the stratospheric ozone layer, the present spectroscopic study focused on spectral transition in UVA, partial UVB and VIS regions. All tested chemicals showed a strong absorption in the UVA/B range, and UV spectral patterns of some tested compounds, including sulisobenzone (**2**), diclofenac Na (**7**), hexachlorophene (**12**) and warfarin Na (**31**), were found to be different between protein-free and albuminous solutions (Fig. 3B, C, D and F). These spectral transitions would be highly indicative of protein binding with these chemicals, and the observations were partly in agreement with previous reports on potent serum protein-binding properties of these chemicals (Gulden *et al.*, 2003; Ji *et al.*, 2002). Although the aROS assay demonstrated the considerable changes in photochemical properties of quinine HCl (**1**) and lomefloxacin HCl (**15**) in the presence of serum albumin, no spectral differences were observed in these chemicals with or without serum albumin (Fig. 3A and E). Thus, there was a data discrepancy between the spectroscopic and photochemical data; therefore, an additional drug-protein interaction study was employed for further characterization.

In order to ensure interaction of chemicals with serum albumin, fluorescence quenching analysis of BSA with or without each chemical was also carried out (Fig. 4). The intrinsic fluorescence intensity of BSA measured before and after the addition of each chemical could provide information on the structural changes of BSA (Kandagal *et al.*, 2006). Theoretically, the fluorescence intensity of a chemical can be decreased by several types of molecular interaction; therefore, the quenching of fluorescence would reflect the molecular interaction. With the addition of some chemicals (**2**, **7**, **12** and **31**) at a concentration of 20 μM , the fluorescence intensity of BSA decreased by c. 19%, 45%, 67% and 21%, respectively. The interaction of a chemical with serum albumin can lead to changes in the dielectric environment of at least one of the two indole moieties at tryptophan residues in BSA as the chromophore may be placed in a more hydrophobic environment (Yuan *et al.*, 1998). There is also the probability that the quenching of BSA by these chemicals is as a result of energy transfer from excited-state tryptophan residues to the bound chemical. A general prerequisite for energy transfer to occur by Förster mechanisms is that the emission band of the donor overlaps the absorption band of the acceptor. Basically, the Förster mechanisms operates through the Coulombic interactions between the donor and the acceptor transition dipoles, and the resonant coupling of the donor and acceptor leads to energy transfer (Chen and Kernohan, 1967). According to the UV spectral data (Fig. 3), all tested chemicals would meet this prerequisite, whereas no fluorescence spectral transitions were observed for quinine HCl (**1**) and lomefloxacin HCl (**15**). In this study, outcomes from the fluorescence experiment were consistent with those from the UV spectral study, and, of all 6 chemicals tested here, 4 chemicals (**2**, **7**, **12**, and **31**) were found to bind with BSA under the current experimental conditions. Previously, plasma protein binding ratios of quinine HCl (**1**) and lomefloxacin

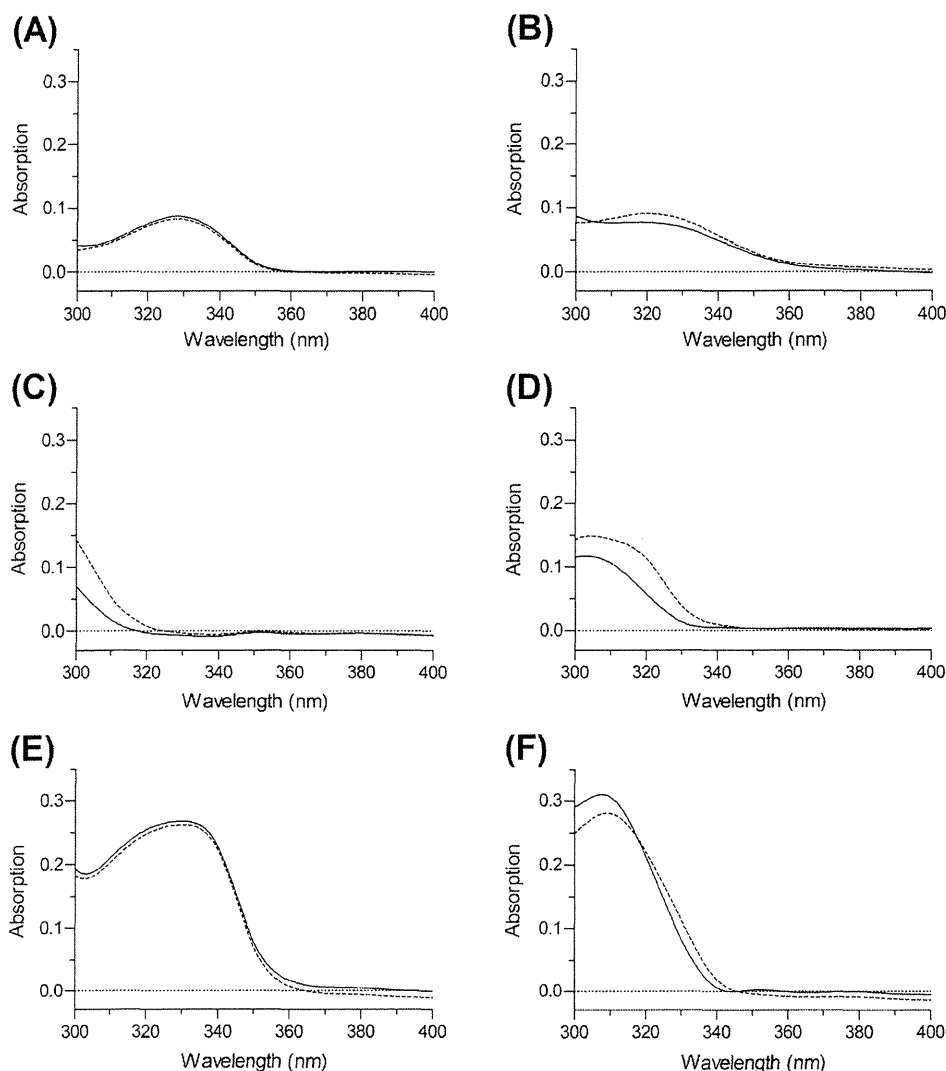


Figure 3. UV/VIS spectral patterns of tested chemicals (20 μ M) with or without an equimolar concentration of bovine serum albumin (BSA) in 20 mM sodium phosphate buffer (pH7.4). (A) quinine HCl (**1**), (B) sulisobenzone (**2**), (C) diclofenac Na (**7**), (D) hexachlorophene (**12**), (E) lomefloxacin HCl (**15**) and (F) warfarin Na (**31**). Solid line, chemical alone; and dashed line, chemical with BSA.

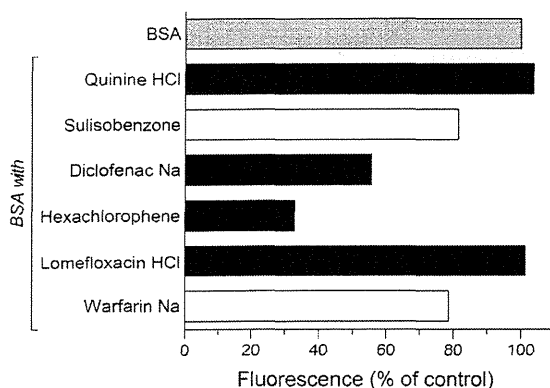


Figure 4. Fluorescence quenching analysis on bovine serum albumin (BSA) (2 μ M) with or without tested chemical (2 μ M). Filled bar, phototoxic chemical; and open bar, non-phototoxic chemical.

HCl (**15**) were determined to be *c.* < 70% and 10%, respectively, whereas the addition of copper ion promoted the interaction of lomefloxacin HCl (**15**) with BSA (Lu *et al.*, 2007). In contrast, 4 chemicals (**2**, **7**, **12** and **31**) exhibited much higher plasma protein binding (>95%) according to the manufacturers' reports, and these previous data would be partly supportive of the present observations. In addition to the binding amount, binding sites of the tested chemicals might also be attributable to the different outcomes from the fluorescence quenching assay.

From these findings, a molecular interaction between chemical and BSA cannot fully explain the changes in ROS generation from some chemicals in albuminous solution. However, the transition in UV spectral patterns and/or fluorescent intensity might be negligible if the chemicals interact with non-chromophore moieties and/or non-fluorescent residues in BSA. Further clarification on the BSA–drug interaction or the possible main effector might be of value to better understand assay limitations and

further modification of the ROS assay to improve the predictability of phototoxic risk and to avoid misleading data.

Conclusion

In the present study, an aROS assay system was developed using an albuminous solution for photosafety assessment under experimental biomimetic conditions. The validation study demonstrated the high robustness of the aROS assay and improved applicability to poorly soluble chemicals. Further assessments on 31 test samples were also indicative of a good predictive capacity of the aROS assay for photosafety evaluation. Comparing outcomes from the ROS assay with those from the aROS assay, the photosensitivity of some chemicals clearly varied in the presence of serum albumin, the mechanism of which might partly involve the molecular interaction. The determination of ROS in the albuminous solution might partly reflect the photochemical behavior of photosensitizers *in vivo*, and the aROS assay system would be more effective to predict the phototoxic potential of pharmaceutical substances with a wide range of applicability.

Acknowledgement

This work was supported in part by a Health Labour Sciences Research Grant from The Ministry of Health, Labour and Welfare, Japan.

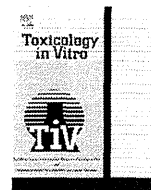
REFERENCES

- Alvarez-Fernandez JG, Castano-Suarez E, Cornejo-Navarro P, de la Fuente EG, Ortiz de Frutos FJ, Iglesias-Diez L. 2000. Photosensitivity induced by oral itraconazole. *J. Eur. Acad. Dermatol. Venereol.* **14**: 501–503.
- Andrade SM, Costa SM. 2008. Ordered self-assembly of protonated porphyrin induced by the aqueous environment of biomimetic systems. *Ann. N. Y. Acad. Sci.* **1130**: 305–313.
- Ashur I, Goldschmidt R, Pinkas I, Salomon Y, Szweczyk G, Sarna T, Scherz A. 2009. Photocatalytic generation of oxygen radicals by the water-soluble bacteriochlorophyll derivative WST11, noncovalently bound to serum albumin. *J. Phys. Chem. A* **113**: 8027–8037.
- Carter DC, Ho JX. 1994. Structure of serum albumin. *Adv. Protein Chem.* **45**: 153–203.
- Chen RF, Kernohan JC. 1967. Combination of bovine carbonic anhydrase with a fluorescent sulfonamide. *J. Biol. Chem.* **242**: 5813–5823.
- Danel C, Foulon C, Goossens JF, Bonte JP, Vaccher C. 2006. Kinetics of racemization of enantiopure N-imidazole derivatives, aromatase inhibitors: studies in organic, aqueous, and biomimetic media. *Tetrahedron-Asymmetry* **17**: 2317–2321.
- Dubakiene R, Kupriene M. 2006. Scientific problems of photosensitivity. *Medicina (Kaunas)* **42**: 619–624.
- Fukuhara A, Nakajima H, Miyamoto Y, Inoue K, Kume S, Lee YH, Noda M, Uchiyama S, Shimamoto S, Nishimura S, Ohkubo T, Goto Y, Takeuchi T, Inui T. 2012. Drug delivery system for poorly water-soluble compounds using lipocalin-type prostaglandin D synthase. *J. Control. Release* **159**: 143–150.
- Gulden M, Morchel S, Seibert H. 2003. Serum albumin binding at cytotoxic concentrations of chemicals as determined with a cell proliferation assay. *Toxicol. Lett.* **137**: 159–168.
- Ji ZS, Li CG, Mao XA, Liu ML, Hu JM. 2002. NMR study on the low-affinity interaction of human serum albumin with diclofenac sodium. *Chem. Pharm. Bull.(Tokyo)* **50**: 1017–1021.
- Jones PA, King AV. 2003. High throughput screening (HTS) for phototoxicity hazard using the *in vitro* 3T3 neutral red uptake assay. *Toxicol. In Vitro* **17**: 703–708.
- Kandagal PB, Ashoka S, Seetharamappa J, Shaikh SM, Jadegoud Y, Ijare OB. 2006. Study of the interaction of an anticancer drug with human and bovine serum albumin: spectroscopic approach. *J. Pharm. Biomed. Anal.* **41**: 393–399.
- Kurono Y, Furukawa A, Takesue Y, Li FL, Ikeda K. 1987. Photo-stabilization and solubilization of an aldose reductase inhibitor, (E)-3-carboxymethyl-5-[(2E)-methyl-3-phenylpropenylidene]rhodani ne (ONO-2235), by human serum albumin. *Chem. Pharm. Bull.(Tokyo)* **35**: 3045–3048.
- Lim HW, Hawk J. 2008. *Photodermatoses*, In *Dermatology*, Bologna JL, Jorizzo JL, Rapini RP (eds). Elsevier: Amsterdam; 1333–1351.
- Lu JQ, Jin F, Sun TQ, Zhou XW. 2007. Multi-spectroscopic study on interaction of bovine serum albumin with lomefloxacin-copper(II) complex. *Int. J. Biol. Macromol.* **40**: 299–304.
- Moore DE. 2002. Drug-induced cutaneous photosensitivity: incidence, mechanism, prevention and management. *Drug Saf.* **25**: 345–372.
- Onoue S, Hosoi K, Wakuri S, Iwase Y, Yamamoto T, Matsuoka N, Nakamura K, Toda T, Takagi H, Osaki N, Matsumoto Y, Kawakami S, Seto Y, Kato M, Yamada S, Ohno Y, Kojima H. 2012. Establishment and intra-/inter-laboratory validation of a standard protocol of reactive oxygen species assay for chemical photosafety evaluation. *J. Appl. Toxicol.* (in press) doi: 10.1002/jat.2776.
- Onoue S, Igarashi N, Yamada S, Tsuda Y. 2008a. High-throughput reactive oxygen species (ROS) assay: An enabling technology for screening the phototoxic potential of pharmaceutical substances. *J. Pharm. Biomed. Anal.* **46**: 187–193.
- Onoue S, Seto Y, Gandy G, Yamada S. 2009. Drug-induced phototoxicity; an early *in vitro* identification of phototoxic potential of new drug entities in drug discovery and development. *Curr. Drug Saf.* **4**: 123–136.
- Onoue S, Tsuda Y. 2006. Analytical studies on the prediction of photosensitive/phototoxic potential of pharmaceutical substances. *Pharm. Res.* **23**: 156–164.
- Onoue S, Yamauchi Y, Kojima T, Igarashi N, Tsuda Y. 2008b. Analytical studies on photochemical behavior of phototoxic substances; effect of detergent additives on singlet oxygen generation. *Pharm. Res.* **25**: 861–868.
- Portes P, Pygmalion MJ, Popovic E, Cottin M, Mariani M. 2002. Use of human reconstituted epidermis Episkin for assessment of weak phototoxic potential of chemical compounds. *Photodermatol. Photoimmunol. Photomed.* **18**: 96–102.
- Quintero B, Miranda MA. 2000. Mechanisms of photosensitization induced by drugs: A generak survey. *Ars Pharmaceutica* **41**: 27–46.
- Rega MF, Reed JC, Pellicchia M. 2007. Robust lanthanide-based assays for the detection of anti-apoptotic Bcl-2-family protein antagonists. *Bioorg. Chem.* **35**: 113–120.
- Selvaag E. 1997. Evaluation of phototoxic properties of oral antidiabetics and diuretics. Photohemolysis model as a screening method for recognizing potential photosensitizing drugs. *Arzneimittelforschung* **47**: 1031–1034.
- Seto Y, Aoki Y, Inoue R, Kojo Y, Kato M, Onoue S, Yamada S. 2011a. Development of dry powder inhaler system for reducing phototoxic risk. In *DDS Conference*, Oku N. (ed.). Biomedical Research Press: Shizuoka; 41–46.
- Seto Y, Hosoi K, Takagi H, Nakamura K, Kojima H, Yamada S, Onoue S. 2012. Exploratory and regulatory assessments on photosafety of new drug entities. *Curr. Drug Saf.* **7**: 140–148.
- Seto Y, Inoue R, Ochi M, Gandy G, Yamada S, Onoue S. 2011b. Combined use of *in vitro* phototoxic assessments and cassette dosing pharmacokinetic study for phototoxicity characterization of fluoroquinolones. *AAPS J.* **13**: 482–492.
- Spielmann H, Balls M, Dupuis J. 1998. The international EU/COLIPA *in vitro* phototoxicity validation study: results of phase II (blind trial). Part 1: the 3T3 NRU phototoxicity test. *Toxicol. In Vitro* **12**: 305–327.
- Stein KR, Scheinfeld NS. 2007. Drug-induced photoallergic and phototoxic reactions. *Expert Opin. Drug Saf.* **6**: 431–443.
- Yuan T, Weljie AM, Vogel HJ. 1998. Tryptophan fluorescence quenching by methionine and selenomethionine residues of calmodulin: orientation of peptide and protein binding. *Biochemistry* **37**: 3187–3195.
- Zhang JH, Chung TD, Oldenburg KR. 1999. A simple statistical parameter for use in evaluation and validation of high throughput screening assays. *J. Biomol. Screen.* **4**: 67–73.



Contents lists available at ScienceDirect

Toxicology in Vitro

journal homepage: www.elsevier.com/locate/toxinvit

Intra-/inter-laboratory validation study on reactive oxygen species assay for chemical photosafety evaluation using two different solar simulators



Satomi Onoue^{a,*}, Kazuhiro Hosoi^b, Tsuguto Toda^c, Hironori Takagi^d, Naoto Osaki^d, Yasuhiro Matsumoto^e, Satoru Kawakami^f, Shinobu Wakuri^g, Yumiko Iwase^h, Toshinobu Yamamotoⁱ, Kazuichi Nakamura^j, Yasuo Ohno^k, Hajime Kojima^l

^a Department of Pharmacokinetics and Pharmacodynamics, School of Pharmaceutical Sciences, University of Shizuoka, 52-1 Yada, Suruga-ku, Shizuoka 422-8526, Japan

^b Non-Clinical Research Group, Ophthalmic Research and Development Center, Santen Pharmaceutical Co., Ltd., 8916-16 Takayama-cho, Ikoma, Nara 630-0101, Japan

^c Drug Developmental Research Laboratories, Shionogi & Co., Ltd., 3-1-1 Futaba-cho, Toyonaka, Osaka 561-0825, Japan

^d Research Center, Taisho Pharmaceutical Co., Ltd., 1-403, Yoshino-cho, Kita-ku, Saitama 331-9530, Japan

^e Safety Research Department, ASKA Pharmaceutical Co., Ltd., 5-36-1, Shimosakunobe, Takatsu-ku, Kawasaki, Kanagawa 213-8522, Japan

^f Pharmaceuticals Research Center, Asahi Kasei Pharma Corporation, 632-1 Mifuku Izunokuni-shi, Shizuoka 410-2321, Japan

^g Laboratory of Cell Toxicology, Hatano Research Institute, Food and Drug Safety Center, 729-5 Ochiai, Hadano, Kanagawa 257-8523, Japan

^h Safety Research Laboratories, Mitsubishi Tanabe Pharma Corporation, 1-1-1, Kazusakamatari, Kisarazu, Chiba 292-0818, Japan

ⁱ Safety Research Laboratories, Mitsubishi Tanabe Pharma Corporation, 2-2-50, Kawaguchi, Toda-shi, Saitama 335-8505, Japan

^j Product Development Regulatory Affairs Department, Shionogi & Co., Ltd., 2-17-5 Shibuya, Shibuya-ku, Tokyo 150-8673, Japan

^k National Institute of Health Sciences (NIHS), 1-18-1 Kamiyoga, Setagaya-ku, Tokyo 158-8501, Japan

^l Japanese Center for the Validation of Alternative Methods (JaCVAM), National Institute of Health Sciences (NIHS), 1-18-1 Kamiyoga, Setagaya-ku, Tokyo 158-8501, Japan

ARTICLE INFO

Article history:

Received 25 September 2013

Accepted 14 November 2013

Available online 30 December 2013

Keywords:

Phototoxicity

Photoreactivity

Reactive oxygen species

Validation

Inter-laboratory precision

ABSTRACT

A previous multi-center validation study demonstrated high transferability and reliability of reactive oxygen species (ROS) assay for photosafety evaluation. The present validation study was undertaken to verify further the applicability of different solar simulators and assay performance. In 7 participating laboratories, 2 standards and 42 coded chemicals, including 23 phototoxins and 19 non-phototoxic drugs/chemicals, were assessed by the ROS assay using two different solar simulators (Atlas Suntest CPS series, 3 labs; and Seric SXL-2500V2, 4 labs). Irradiation conditions could be optimized using quinine and sulisobenzonate as positive and negative standards to offer consistent assay outcomes. In both solar simulators, the intra- and inter-day precisions (coefficient of variation; CV) for quinine were found to be below 10%. The inter-laboratory CV for quinine averaged 15.4% (Atlas Suntest CPS) and 13.2% (Seric SXL-2500V2) for singlet oxygen and 17.0% (Atlas Suntest CPS) and 7.1% (Seric SXL-2500V2) for superoxide, suggesting high inter-laboratory reproducibility even though different solar simulators were employed for the ROS assay. In the ROS assay on 42 coded chemicals, some chemicals (ca. 19–29%) were unevaluable because of limited solubility and spectral interference. Although several false positives appeared with positive predictivity of ca. 76–92% (Atlas Suntest CPS) and ca. 75–84% (Seric SXL-2500V2), there were no false negative predictions in both solar simulators. A multi-center validation study on the ROS assay demonstrated satisfactory transferability, accuracy, precision, and predictivity, as well as the availability of other solar simulators.

© 2013 Elsevier Ltd. All rights reserved.

Abbreviations: 3T3 NRU PT, 3T3 neutral red uptake phototoxicity test; 8-MOP, 8-methoxypsoralen; CV, coefficient of variation; ECVAM, Europe Center for the Validation of Alternative Methods; GLP, Good Laboratory Practice; ICCVAM, Interagency Coordinating Committee on the Validation of Alternative Methods; JaCVAM, Japanese Center for the Validation of Alternative Methods; KoCVAM, Korean Center for the Validation of Alternative Methods; OECD, Organisation for Economic Co-operation and Development; PABA, p-aminobenzoic acid; ROS, reactive oxygen species; SDS, sodium dodecyl sulfate; UV, ultraviolet; VIS light, visible light; VMT, Validation Management Team; ZEBET, International Centre for Documentation and Evaluation of Alternative Methods to Animal Experiments.

* Corresponding author. Tel.: +81 54 264 5633; fax: +81 54 264 5635.

E-mail address: sonoue@u-shizuoka-ken.ac.jp (S. Onoue).

1. Introduction

Drug-induced phototoxicity can appear in light-exposed tissues, elicited by topical or systemic application of drugs and exposure to sunlight or artificial light (Moore, 2002). Several classes of pharmaceuticals cause phototoxic reactions in skin and/or eyes (Moore, 1998, 2002), including photoirritant, photoallergic, and photogenotoxic events (Epstein, 1983). Although drug-induced phototoxicity might not be a life-threatening side effect in most cases, phototoxicity has a major impact on quality of life and therapeutic compliance/outcomes. With the aim of reducing and

preventing phototoxicity, increasing attention has been drawn to hazard identification and risk management upon photosafety assessment of pharmaceutical products. A number of *in vitro* methodologies have been developed for photosafety assessment over the past few years. Guidance on the photosafety testing of medicinal products was established by regulatory agencies in the US and EU in the early 2000s (Seto et al., 2012), and the recent issuance of the draft ICH S10 photosafety guidance document also provided a detailed framework and guidance for photosafety evaluation of pharmaceutical substances and products (ICH, 2013). These guidelines describe photosafety assessment strategies on the basis of photochemical and photobiochemical properties, and *in vivo* pharmacokinetic behavior (EMEA/CPMP, 2002; FDA/CDER, 2002; OECD, 2004).

Previously, a reactive oxygen species (ROS) assay was developed for the photosafety assessment of pharmaceutical substances (Onoue et al., 2008b; Onoue and Tsuda, 2006), in which the generation of ROS such as singlet oxygen and superoxide from photoirradiated chemicals was monitored. The photo-excited phototoxins tend to generate ROS, triggering phototoxic events in the light-exposed tissues (Brendler-Schwaab et al., 2004; Epstein and Wintroub, 1985), and the photobiochemical responses of phototoxins could provide a rationale for the use of ROS assay in photosafety assessment. A multi-center validation study was previously carried out to establish and validate a standard protocol for the ROS assay, supervised by the Japanese Center for the Validation of Alternative Methods (JaCVAM) (Onoue et al., 2013). Outcomes from the validation study were indicative of the satisfactory transferability, inter-laboratory variability, and predictivity of the ROS assay, and these findings provided sufficient support for the ROS assay as an alternative method for photosafety assessment. However, the ROS assay in the previous validation study was conducted in only one solar simulator (Atlas Suntest CPS series), so the applicability of other solar simulators to the ROS assay has never been elucidated.

The present study was designed to validate a standard protocol for the ROS assay using different solar simulators, under the supervision of the Japanese Center for the Validation of Alternative Methods (JaCVAM) throughout the work. Since a UVA light source has been widely employed for the 3T3 neutral red uptake phototoxicity test (3T3 NRU PT) (Spielmann et al., 1994b), the present validation study focused on the compatibility of another solar simulator (Seric SXL-2500V2) commonly used for 3T3 NRU PT as an alternative to the Atlas Suntest series. In accordance with the previous study design, inter- and intra-laboratory validation studies were carried out to assess the transferability, assay precision, and predictive capacity of the ROS assay using 2 standard chemicals and 42 coded chemicals, including 23 phototoxins and 19 non-phototoxic drugs/chemicals.

2. Materials and methods

2.1. General conditions of the study

The validation study was coordinated as reported previously (Onoue et al., 2013). Briefly, the Validation Management Team (VMT) was organized under the JaCVAM, and the roles of the VMT were to design the study, to guide and facilitate the validation process, to evaluate the results and, on the basis of these, render subsequent decisions during the progress of the study, and to analyze the outcomes from the studies. The VMT was comprised of the trial coordinator, assistant trial coordinator, chemical management group, data analysis group, quality assurance group, and representatives of participating laboratories. The validation study and the quality assurance were carried out in the spirit of Good Laboratory Practice (GLP), although not all the participating laboratories

routinely worked under GLP certification in accordance with the protocol provided by the VMT. All raw data and the data analysis sheet were pre-checked for quality in each laboratory and then reviewed by the quality assurance group of the VMT.

2.2. Participating laboratories

The seven participating laboratories are as follows: Laboratory 1 (Lab#1), Mitsubishi Tanabe Pharma Corporation, Safety Research Laboratories; Laboratory 2 (Lab#2), Food and Drug Safety Center, Hatano Research Institute; Laboratory 3 (Lab#3, lead laboratory), University of Shizuoka, School of Pharmaceutical Sciences; Laboratory 4 (Lab#4), Asahi Kasei Pharma Corporation, Pharmaceuticals Research Center; Laboratory 5 (Lab#5), ASKA Pharmaceutical Co., Ltd., Safety Research Department; Laboratory 6 (Lab#6), Shionogi & Co., Ltd., Drug Developmental Research Laboratories; and Laboratory 7 (Lab#7), Taisho Pharmaceutical Co., Ltd., Pharmaceutical Technology Laboratories.

2.3. Chemicals and reagents

As reported previously, chemicals for the validation study were selected by the chemical management group of the VMT in cooperation with Dr. Manfred Liebsch (ZEBET), Europe Center for the Validation of Alternative Methods (ECVAM), Interagency Coordinating Committee on the Validation of Alternative Methods (ICCVAM), and Korean Center for the Validation of Alternative Methods (KoCVAM). According to the reported *in vitro/in vivo* photosafety information and clinical observations (Durbize et al., 2003; Moore, 2002; Motley and Reynolds, 1989; Onoue et al., 2010; Peters and Holzhtuter, 2002; Portes et al., 2002; Spielmann, 1994; Spielmann et al., 1994a, 1998a,b, 1995; Trevisi et al., 1994) and in-house assay results from *in vitro* 3T3 NRU PT, 2 standard chemicals and 42 test chemicals, including 23 phototoxins and 19 non-phototoxic drugs/chemicals, were selected (Table 1).

Quinine (**1**), chlorpromazine HCl (**6**), fenofibrate (**8**), ketoprofen (**10**), 6-methylcoumarin (**11**), nalidixic acid (**13**), norfloxacin (**15**), ofloxacin (**16**), piroxicam (**17**), promethazine HCl (**18**), anthracene (**21**), rose bengal (**25**), aspirin (**26**), benzocaine (**27**), erythromycin (**28**), phenytoin (**29**), penicillin G (**30**), cinnamic acid (**34**), L-histidine (**36**), 2-(2*H*-benzotriazol-2-yl)-4-(1,1,3,3-tetramethylbutyl)phenol (ocritazole, **38**), octyl methacrylate (**39**), *p*-aminobenzoic acid (PABA, **42**), sodium dodecyl sulfate (SDS, **43**), NaH₂PO₄·2H₂O, Na₂HPO₄·12H₂O, dimethyl sulfoxide (DMSO), *p*-nitrosodimethylaniline, imidazole, and nitroblue tetrazolium (NBT) were obtained from Wako Pure Chemical Industries (Osaka, Japan). Doxycycline HCl (**7**) and nalidixic acid (Na salt) (**14**) were bought from MP Biomedicals (Irvine, CA, USA). Rosiglitazone (**19**) and methylbenzylidene camphor (**37**) were purchased from Enzo Life Sciences International (Farmingdale, NY, USA) and Alfa Aesar (Ward Hill, MA, USA), respectively. Sulisobenzone (**2**), acridine HCl (**4**), furosemide (**9**), 8-methoxypsoralen (**12**), avobenzene (**22**), hexachlorophene (**24**), octyl methoxycinnamate (**40**), and octyl salicylate (**41**) were purchased from Tokyo Chemical Industry (Tokyo, Japan). Acridine (**3**), amiodarone HCl (**5**), 6-methylcoumarin (**11**), tetracycline (**20**), bithionol (**23**), 2-*tert*-butyl-6-(5-chloro-2*H*-benzotriazol-2-yl)-4-methylphenol (bumetizole, **31**), camphor sulfonic acid (**32**), chlorhexidine (**33**), 2-(2-hydroxy-5-methylphenyl)benzotriazole (drometizole, **35**), and 2-(2*H*-benzotriazol-2-yl)-6-dodecyl-4-methylphenol (UV-571, **44**) were purchased from Sigma–Aldrich Japan (Tokyo, Japan). A quartz reaction container for high-throughput ROS assay (Onoue et al., 2008a) was constructed by Ozawa Science (Aichi, Japan).

Each chemical for the validation study was supplied from the VMT to participating laboratories. Quinine (**1**), a positive control, and sulisobenzone (**2**), a negative control, were uncoded, and the